ARMY RESEARCH LABORATORY

Polystyrene/Hyperbranched Polyester Blends and Reactive Polystyrene/Hyperbranched Polyester Blends

by Thomas J. Mulkern and Nora C. Beck Tan

ARL-TR-1876   January 1999

Preceding Page Blank

DTIC QUALITY INSPECTED 2

The findings in this report are not to be construed as an official
Department of the Army position unless so designated by other
authorized documents.

Citation of manufacturer's or trade names does not constitute an
official endorsement or approval of the use thereof.

Destroy this report when it is no longer needed. Do not return
it to the originator.

Army Research Laboratory

Aberdeen Proving Ground, MD 21005-5069

Polystyrene/Hyperbranched Polyester Blends and Reactive Polystyrene/Hyperbranched Polyester Blends

Thomas J. Mulkern and Nora C. Beck Tan
Weapons and Materials Research Directorate, ARL

Abstract

Newly developed hyperbranched polyols (HBP) possess a highly branched three-dimensional structure and a high density of functional end groups relative to conventional linear or branched polymer molecules. Due to their inherent low viscosity and versatile end group chemistry, these materials are attractive as polymer blend modifiers for improved processing as well as improved properties due to reactive compatibilization. In this work, the incorporation of HBPs in thermoplastic blends was investigated. Several volume fractions of hydroxyl functionalized hyperbranched polyesters were melt blended with nonreactive polystyrene (PS) and two types of reactive styrene maleic anhydride (SMA). Rheological data proved that HBPs are effective processing aids in both nonreactive and reactive blends. Studies including microscopy, thermal analysis, dynamic mechanical analysis, and Fourier transform infrared (FTIR) indicate that PS and HBP form an immiscible blend, while SMA and HBP form compatibilized blends. The degree of compatibilization in the blends was found to increase with SMA reactivity.

Table of Contents

List of Figures

vi

List of Tables

1. Historical Background and Introduction

1.1 Polymer Blends. The research into the development of polymer blends has increased significantly in the past several decades, predominantly for economic reasons. Polymer alloys and blends make up about 30% of polymer consumption with an annual growth rate of about 9% per year for the past decade. This is about four times the growth rate of the polymer industry as a whole [1]. This growth is primarily due to the cost involved for research, development, and marketing a new homopolymer.

The competition in the polymer industry is fierce, and the availability of new niche markets for these polymers is small. Therefore, it is attractive to produce polymer blends with a balance of desirable properties contributed by each component. The successful blending of existing polymers reduces the cost or need of developing new homopolymers.

1.2 Blend Miscibility. A polymer blend is made up of an intimate combination of two or more homopolymer chains of chemically or structurally different features, which are not covalently bonded to each other [2]. At equilibrium, a polymer blend may exist in a single phase of two intimately mixed polymer molecules or in a multiphase system where each phase is made of predominantly one individual component. The former is called a miscible blend, while the latter is referred to as an immiscible blend.

The Gibbs free energy of mixing, ΔG_{mix}, governs the equilibrium phase behavior of a polymer blend:

$$\Delta G_{mix} = \Delta H_{mix} - T\,\Delta S_{mix}, \tag{1}$$

where ΔH_{mix} is the heat of mixing, ΔS_{mix} is the entropy of mixing, and T is absolute temperature. The conditions for miscibility are

$$\Delta G_{mix} < 0$$

1

and

$$(\partial^2 \Delta G_{mix}/\partial \phi_i{}^2)_{TP} > 0,$$

where ϕ_i is the volume fraction of component i in the mixture, T is absolute temperature, and P is pressure. In most polymer blends, ΔS_{mix} is very small and ΔH_{mix} is positive; this results in a positive value for ΔG_{mix}. As a result, the two polymers are immiscible and a multiphase morphology is observed [2, 3].

In an immiscible system blend, well-defined phases are typically produced with poor interfacial mechanical properties. The presence of poor mechanical properties is due to the low interfacial adhesion between the phases as well as the size, shape, and distribution of the second-phase particles in the matrix material [4, 5].

1.3 Compatibilizers. Immiscible blends need compatibilization for improved performance. Poor mechanical properties in immiscible blends are due primarily to the poor interfacial adhesion between the phases as well as coarse blend morphology [6, 7]. Typically, several requirements must be satisfied in order to see an improvement. First, a reduction in the interfacial tension, which facilitates dispersion, must occur. Second, the morphology should be stabilized against high-stress processing. Third, the adhesion between the phases in the solid state must be enhanced, thereby improving the mechanical properties of the blend. These requirements of the morphology and mechanical properties of immiscible blends may be met with the addition of compatibilizers [8].

Most compatibilizers consist of block or graft copolymers. Block or graft copolymers are derived from two or more homopolymers of chemically or structurally different features that are covalently bonded at some point along the backbone. In a block copolymer, these homopolymer segments appear in an alternating fashion along a linear copolymer backbone (Figure 1).

A-A-A-B-B-B-B-A-A-B-B-B-B-A

Figure 1. Block Copolymer.

2

In a graft copolymer, these segments appear as side chains attached to a homopolymer backbone (Figure 2).

```
  B        B              B
  B        B              B
  B        B              B
A-A-A-A-A-A-A-A-A-A-A-A-A
     B            B         B
     B            B         B
     B            B         B
```
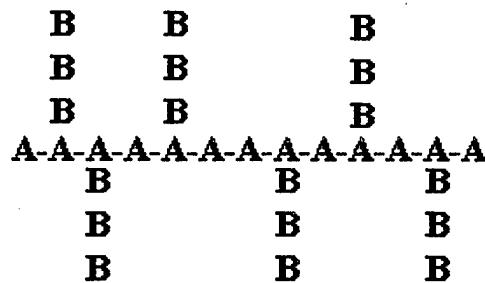
Figure 2. Graft Copolymer.

Each segment of the compatibilizer is miscible in one phase of the polymer blend. An immiscible blend of polymer A and B may be compatibilized by the addition of type A-B copolymers or by type X-Y copolymers where the X segment is miscible in polymer A but not miscible in polymer B, and vice versa (Figure 3).

Polymer A   Compatibilizers   Polymer B
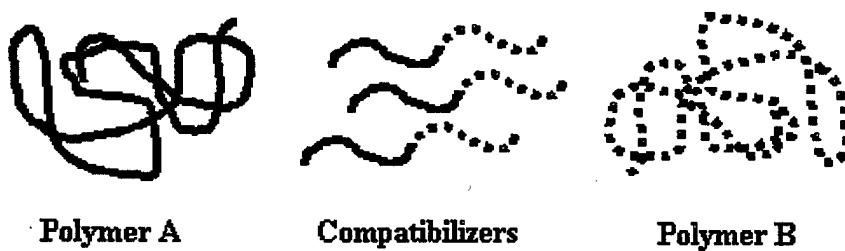
Figure 3. Schematic of Compatibilizer.

The compatibilizers segregate to the interfaces in a blend and become entangled in both phases, stabilizing the dispersion and mechanically reinforcing the interface (Figure 4). Compatibilizers may act as surfactants or as agents that inhibit coalescence during processing, resulting in a refinement of the blend morphology.

Polymer A   Polymer B

Figure 4. Schematic of Compatibilizer at the Interface of a Polymer Blend.

Compatibilizers have been shown to dramatically improve the interfacial bonding and the mechanical properties of immiscible blends when present only in small amounts [9–11]. Copolymer compatibilizers may be produced in a separate step and added to the blend during processing or produced in situ using a reactive processing scheme.

1.4 Reactive Compatibilization. Reactive extrusion, reactive processing, or reactive compounding all refer to a process by which chemical reactions take place during a melt/mix processing of polymers. In such a case, the processing equipment is utilized as a chemical reactor to form compatibilizers as well as a processing tool [12–14]. An understanding of the ongoing reaction mechanisms is crucial for successful reactive processing. The residence time is critical in the reactive extrusion process. Sufficient time must be allowed in order for the reaction to take place in the extruder. Conversely, the reaction must not take place too soon, since a premature reaction may cease or break the mixing elements and cause serious damage to the mixer. The residence time is determined by several variables including the materials, mixer type, and operating speed.

An example of reactive processing involved blending PE grafted with dimethlyamino ethyl methacrylate (DMAEMA) with styrene-maleic anhydride (SMA). This was performed to illustrate the improved compatibility when compared to a blend with pure PE [15]. Blends containing pure PE, grafted PE (G-PE), and SMA were prepared by varying the pure PE content of 10%, 30%, and 50%. Sample morphology studies, Fourier transform infrared (FTIR) analysis, and thermal analysis showed that the G-PE/SMA blend was more miscible and resulted in better fracture toughness than a pure PE/SMA blend. This improved compatibility can be attributed to

4

the change in interfacial tension between the PE and polystyrene phases. This was brought about by the chemical interaction between the acidic anhydride groups in the polystyrene phase and the basic DMAEMA groups grafted on the PE.

Compatibilizers may also be formed in situ during a reactive mixing process. Copolymer formation during reactive processing is particularly useful since compatibilizers are economically formed. Cost savings are apparent when a processing step is eliminated; if a compatibilizer can be made during processing, it does not need to be made separately and added to the system.

The fundamental requirements for compatibilization are to allow sufficient mixing in order to achieve the desired dispersion of one polymer in another, to provide functional groups that are capable of reacting across an interface and reacting within the residence time in the mixer, and to ensure that the bonds formed during reaction are stable for future processing operations [16]. Extensive research has been performed in the last several years in the area of reactive polymer blend processing [17–20], during which compatibilizers are formed in the process proving economic benefit.

1.5 Hyperbranched Polymers. The dendritic family of polymers [21] consists of several molecular structures that represent a fourth major class of polymer architecture (Figure 5), characterized by a repetitive branching structure. Dendritic polymer molecules were first conceptualized in the 1950s [22] but were not successfully synthesized until the early 1980s by Dow Chemical [23, 24].

Recently, dozens of patents have been filed on the structure and synthesis [25–36] of dendritic polymers. Other areas of interest for these materials include the biomedical field for gene therapy and drug delivery applications [37–49]. Patents have been filed by industries having a desire for low-viscosity fluids for coatings, inks, glues, or lubrication applications [50–56]. Several patents are filed for common household goods such as cosmetics or laundry

MOLECULAR ARCHITECTURE

LINEAR   BRANCHED   CROSS LINKED   DENDRITIC
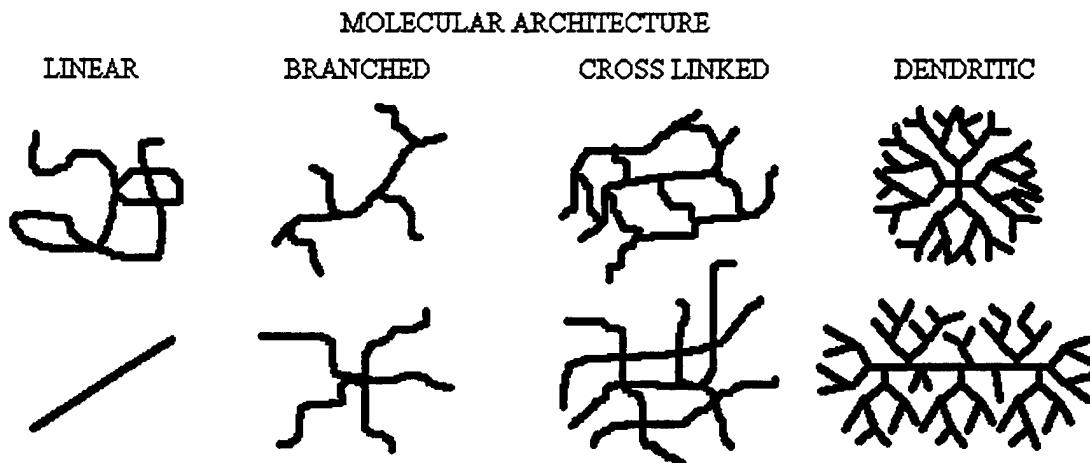
Figure 5. Four Major Molecular Architectures.

detergent. These unique materials also have potential to be used as modifiers to improve processing or mechanical properties in material science applications [57–61].

The polymer architectures within this family vary from perfect monodisperse structures, which are called dendrimers, to the hyperbranched polymer molecules examined in this study, which are not perfect structures and have a polydispersity of greater than two. The size of the dendrimer molecule can be precisely controlled depending on the synthesis approach [62]. Typically, the lower the polydispersity, the higher the cost of synthesis. Due to the high cost of synthesis and subsequent lack of availability, dendritic polymers did not come into widespread study until the mid 1990s. New lower cost synthesis of these hyperbranched polymer molecules has allowed further research into structure, properties, and the potentially endless list of applications [63–65].

The highly branched molecules are different from traditional branched polymers due to the degree of branching. Branched polymers typically consist of a linear backbone with random long or random short linear side chains. Hyperbranched polymers branch out from a central core or backbone and grow in a radial fashion (Figure 6).

6

GENERATION 1   GENERATION 2   GENERATION 3   GENERATION 4
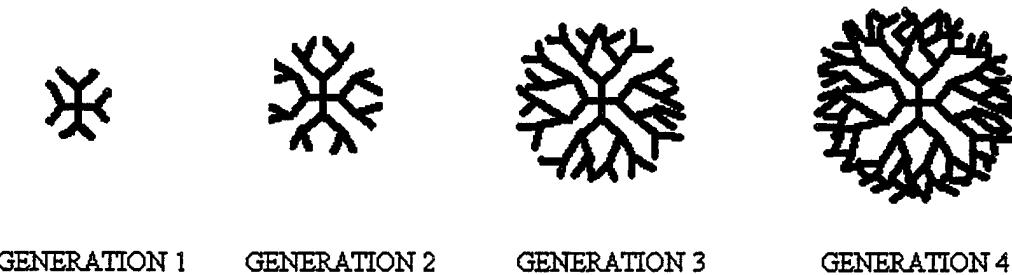
Figure 6. Generation Growth of Dendritic Polymer Molecule.

Each branch splits to form two new branches; these branches each split again to form two more branches. Every time these branches split, the number of surface repeat units doubles, increasing the density of the outer shell, which, in turn, greatly increases the amount of functional end groups available on the surface. Roughly, half of the repeat units present in the hyperbranched polymer molecule are functional (Figure 7) compared to the two functional groups present in an end terminated linear polymer molecule.
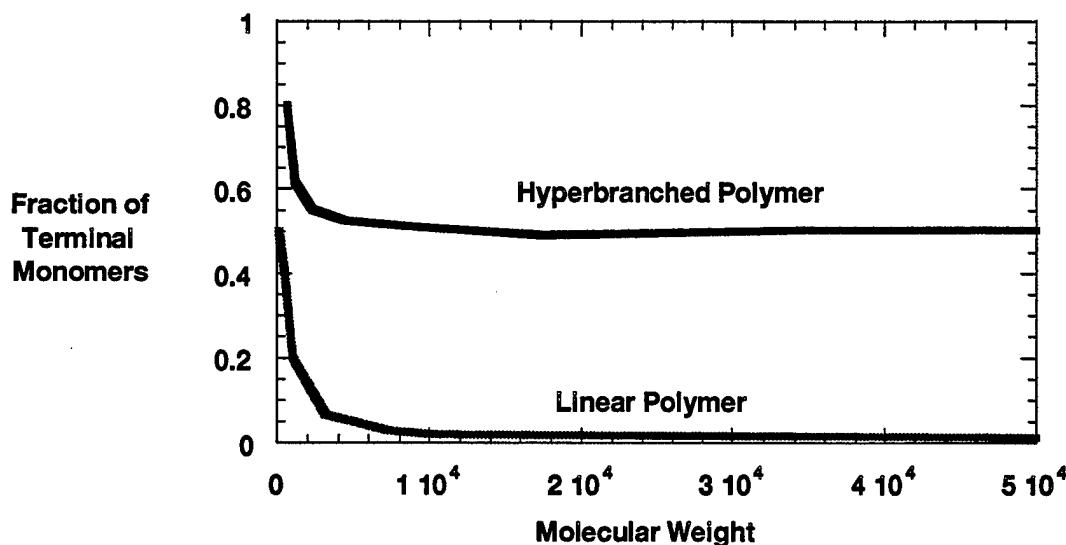
Figure 7. Fraction of Terminal Monomers.

Dendrimer interiors and surfaces can be readily modified to possess chemically reactive or passive functional groups. The inherently low density of the dendrimer core and resulting empty cavities may be used to encapsulate substances for a given application. Surface modification

7

may allow for the addition of reactive and/or inert moieties on the outer shell for a desired degree of reactivity/solubility and subsequent release of encapsulated substances. Surface modification allows every known bonding mode to be integrated onto the surface of this precisely controlled nanoscopic structure [66]. Dendrimer surfaces can be modified with electrophilic or nucleophilic, hydrophilic or hydrophobic, and cationic or anionic moieties. This allows selective compatibility, reactivity, and solubility at each generation if desired.

Hyperbranched polymers show promise in several areas due to their unique molecular architecture. The three-dimensional structure differs from conventional linear and branched polymer molecules in that the density of repeat units per volume is extremely high (Figure 8).
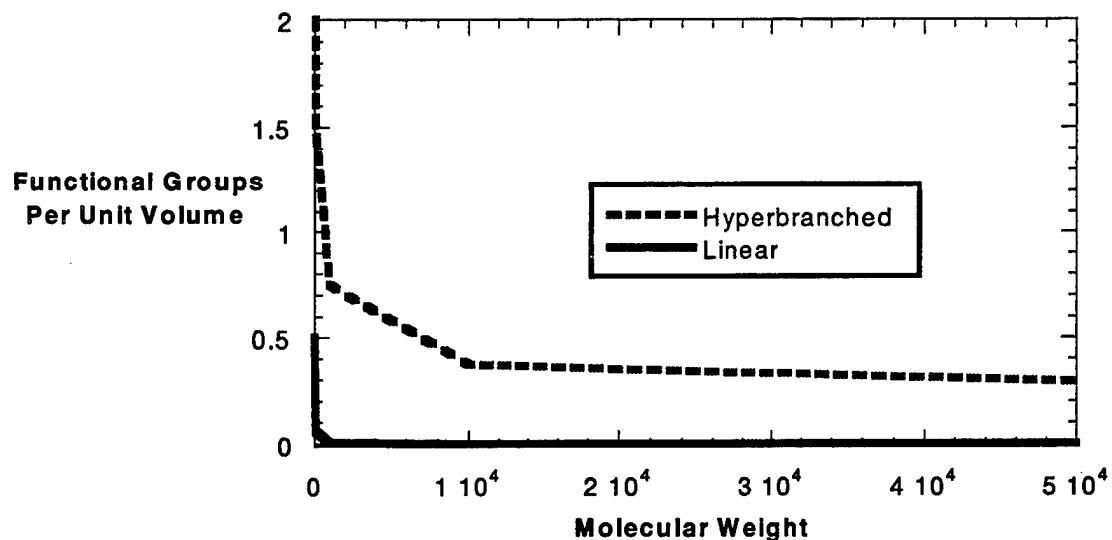
Figure 8. Density of Functional Groups Per Volume.

The structures mimic the hydrodynamic volume of spheres in solution or in the melt as the molecules easily flow past each other under an applied shear stress (Figure 9). This results in a low melt viscosity, even at extremely high molecular weights due to a lack of restrictive interchain entanglements. Even at a high molecular weight, the molecules exhibit an order of magnitude drop solution viscosity or in melt viscosity when compared to linear analogues [67, 68]. Thus, dendritic polymers should prove to be an excellent processing aid due to the molecular structure.
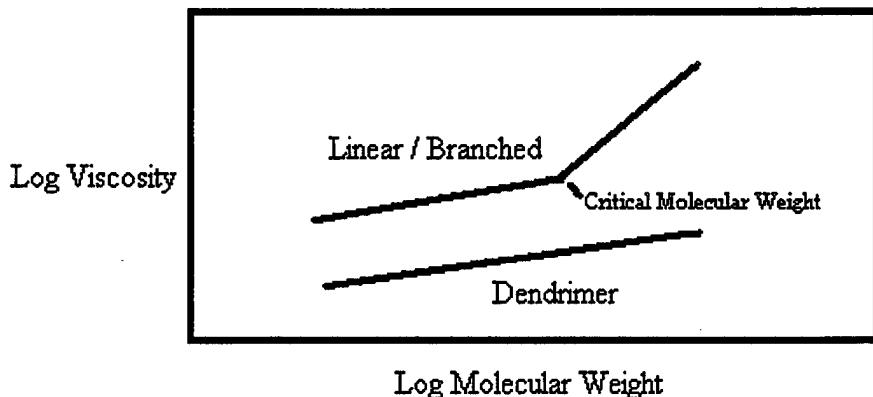
Figure 9. Viscosity vs. Molecular Weight.

The viscosity of dendrimer materials is not like that of linear or branched polymer molecules. Even at a high molecular weight, Newtonian viscosity behavior is observed at all shear rates due to the lack of chain entanglement [69]. The presence of shear thinning (Figure 10) observed at high shear rates in linear and branched polymers is not apparent in viscosity measurements for dendritic polymers [67].
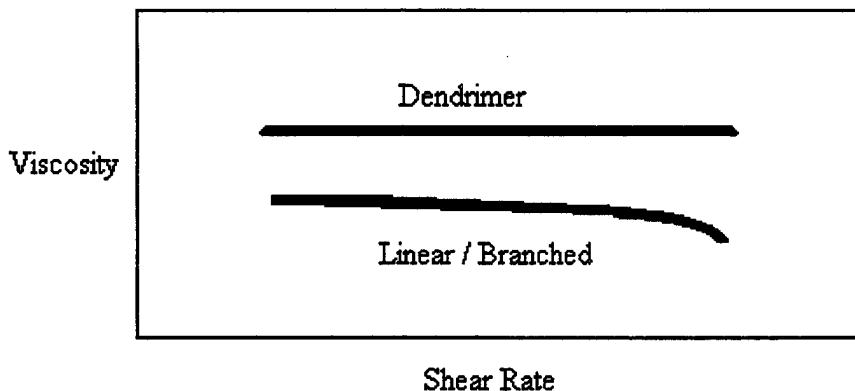
Figure 10. Newtonian vs. Non-Newtonian Rheological Behavior.

Dendritic polymers are a natural for use as a blend additive for the reasons mentioned previously. An end-group chemistry that can be tailored to a specific reactivity or compatibility is attractive for reactive processing. The unique highly branched architecture promotes a low viscosity at all shear rates.

1.6 Hyperbranched Polymer Blends. As previously mentioned, polymers are generally immiscible in each other. Therefore, when blended, a two-phase material with well-defined boundaries is produced, typically with poor mechanical properties. When using hyperbranched polymers in a blend, the inherent problem of polymer/polymer immiscibility also comes into play. This immiscibility in polymer blends may be attributed to the chemistry of the materials blended and not the architecture. A recent study examines the miscibility of hyperbranched polymers with linear analogues [70] where structure as well as chemical composition may play a roll in the miscibility or lack of miscibility.

Another study demonstrated the use of hyperbranched polymers as a processing aid [68]. Hyperbranched polymers and linear analogues were melt blended at several concentrations, resulting in a 10-fold decrease in complex viscosity at all temperatures and shear rates. The authors suggest that this may be due to the migration of hyperbranched polymer to the surface of the bulk polymer. A nonreactive system was studied; the molecular structure of the hyperbranched polymer allowed essentially unrestricted mobility among the linear molecules, and the dendritic molecules that migrated to the surface acted as a lubricant.

Recent work has also been published describing successful incorporation of these hyperbranched polyols (HBPs) as tougheners in an epoxy resin system without an increase in the viscosity typically seen in conventional toughened thermoset resins [71, 72]. The addition of 5% HBP by weight to a carbon fiber-reinforced epoxy system increased the critical energy release rate, G_{Ic}, from 1,400 J/m^2 to 2,500 J/m^2. Similar results were achieved with a glass-reinforced epoxy system, where G_{Ic} increased from 500 J/m^2 to 1,150 J/m^2.

To date, no studies have been conducted on the use of HBPs as tougheners in a reactively compatibilized thermoplastic blend. The high number of functional groups on the densely packed outer shell of the hyperbranched polymers makes them an attractive candidate for reactive processing. The HBP surface groups may react with a functionalized homopolymer and produce compatibilizers in situ.

The scope of this research is to study and attempt to take advantage of these hyperbranched polymers' truly unique structural and reactive properties to produce superior thermoplastic polymer blends.

Through reactive compatibilization, we hope to create thermoplastic polymer blends with improved interfacial adhesion and refined morphology. The resulting morphology, mechanical properties, and processing characteristics are examined. If an improvement in mechanical properties can be achieved while at the same time improving the processing characteristics of HBP blends, the benefits of these novel polymers will be demonstrated.

2. Experimental Materials, Processing, and Methodology

2.1 Materials. A nonreactive polystyrene (PS) and two reactive SMA resins with different maleic anhydride (MA) content were chosen for melt blending with an HBP having hydroxyl terminated end groups. The manufacturer's data is presented in Table 1.

Table 1. Resin Data

Materials	Mw (g/mol)	Mn (g/mol)	Mw/Mn	Melt Flow (g/10 min)	Density (g/cm^2)
PS	300,000	115,000	2.60	1.50	1.04
SMA1	200,000	100,000	2.00	1.90	1.10
SMA2	180,000	90,000	2.00	1.90	1.08
HBP[a]	7,300	—	2.00	—	1.30

[a] Theoretical.

Fourth-generation (G4) Perstorp HBPs are developmental hyperbranched polyester molecules with 64–OH terminated end groups per molecule. The HBP G4 molecules (Figure 11) consist of a pentaerythritol ($C_5H_{12}O_4$) core and multiple 2,2 dimethylol propionic acid ($C_5H_{10}O_4$) chain extenders or repeat units.

11

Core

Chain Extender

Pentaerythritol   2,2 - Dimethylol propionic acid
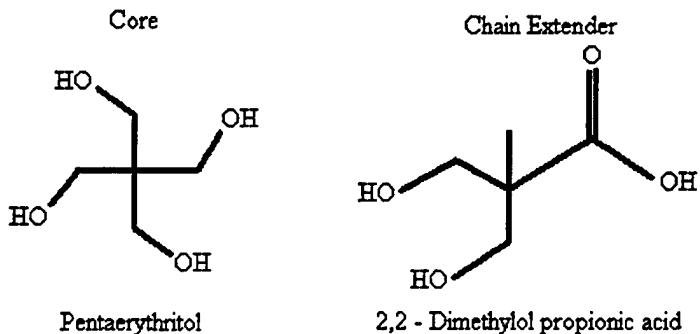
Figure 11. HBP Building Blocks.

These materials were supplied in small quantities with little technical data. The developmental resins are now commercially available in small quantities under the trade name of Boltorn [73].

The two types of SMA random copolymer (Figure 12) produced by ARCO are Dylark 232 (SMA1) and Dylark 332 (SMA2), respectively [74]. Both materials are general-purpose transparent-grade resins. Based on elemental analysis performed by Lehigh Testing Services of New Castle, DE, and the manufacturer's data, the number of functional groups per molecule were determined. SMA1 contained 9.11% MA by weight, and SMA2 contained 13.9% MA by weight.
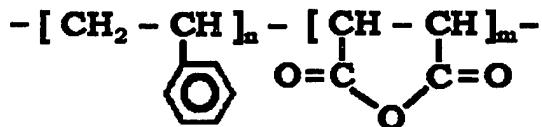
Figure 12. Styrene Maleic Anhydride Repeat Unit.

The PS (Figure 13) resin, Styron 685D [75], manufactured by Dow Chemical is a general-purpose transparent grade of resin.

Several publications cite the use of SMA as part of a practical compatibilized or reactively compatibilized blend [76–81]. In this co-reactive system, a ring opening reaction takes place

12

$$-[\ CH_2 - CH \ ]_n-$$
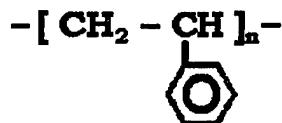
Figure 13. Polystyrene Repeat Unit.

(Figure 14) on the SMA resulting in an acid and ester functionality, which reacts with the –OH functional groups on the HBP.
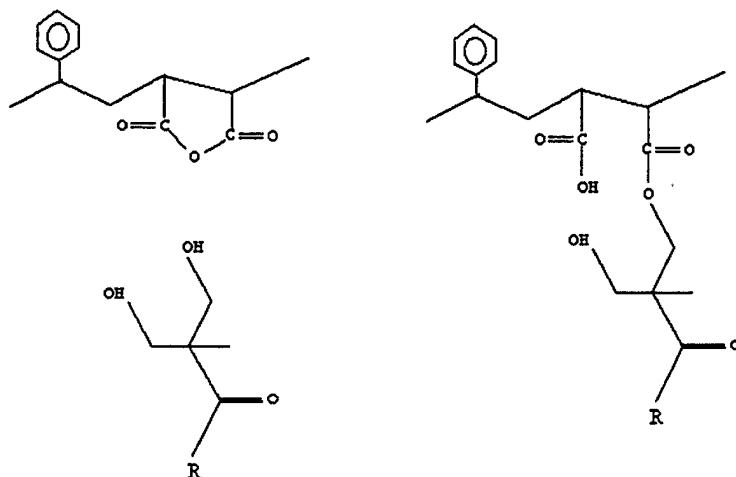
Figure 14. Expected Reaction Between SMA and HBP.

Covalent bonds are formed between the two polymer molecules and copolymer compatibilizers are formed. An improved morphology consisting of a refined microstructure with small, evenly dispersed second-phase particles should be evident when compared to noncompatibilized blends of the same homopolymers.

2.2 Polymer Blends. Reactive blending was chosen as a mechanism to form in situ compatibilized polymer blends. Nine polymer blends and three controls were prepared by varying the concentration of HBP in each. PS, SMA1, and SMA2 materials were blended with 0%, 2%, 5%, and 10% HBP by weight. The 10% blends were fully characterized. The highest concentration of HBP that could be blended in the batch mixer was 10% by weight due to the mismatch in viscosity between the matrix material and the HBP polymers as well as the

13

limitations of the processing equipment. Blends with higher loading of HBP may be attained with the use of a twin screw extruder.

For each of the blends prepared, the number of functional groups on the PS, SMA, and HBP (Table 2) for a given mass of polymer along with the ratio of reactive groups present were determined. In the SMA1/HBP blends, there was an excess of MA functional groups in the 2% and 5% blends but there was an excess of HBP hydroxy functional groups in the 10% blend. There was an excess of MA functional groups in all of the SMA2/HBP blends. There were no functional groups on the PS to react with the HBP hydroxy functional groups in the PS/HBP blends.

Table 2. Number of Functional Groups Present in the SMA/HBP and PS/HBP Blends

Blends	Matrix (g)	No. MA Groups	HBP (g)	No. $-$OH Groups[a]	MA/$-$OH
SMA1-2	65.00	3.64E+22	1.30	6.91E+21	5.27
SMA1-5	65.00	3.64E+22	3.50	1.86E+22	1.96
SMA1-10	64.00	3.58E+22	7.00	3.72E+22	0.96
SMA2-2	65.00	5.47E+22	1.30	6.91E+21	7.92
SMA2-5	65.00	5.47E+22	3.50	1.86E+22	2.94
SMA2-10	64.00	5.39E+22	7.00	3.72E+22	1.45
PS-2	65.00	9.99E+00	1.30	6.91E+21	0.00
PS-5	65.00	9.99E+00	3.50	1.86E+22	0.00
PS-10	64.00	0.00E+00	7.00	3.72E+22	0.00

[a] Based on theoretical data.

The PS and HBP are not coreactive and will form an immiscible blend when mixed. Reactive compatibilization will be in the SMA/HBP blends due to ring-opening reactions that take place between the MA on the SMA and hydroxyl functional group on the HBP.

2.3 Processing. Several attempts at blending these materials were made using different types of processing equipment including a CSI Max Mixing extruder and the Haake Polylab system equipped with a single-screw extruder.

A batch mixing process was ultimately adopted to process the blends. The blends were mixed in small batches of approximately 65 g in the Haake Rheomix 600 mixer driven by a Haake Rheocord 40 system. The mixing chamber specifications are listed in Table 3.

Table 3. Mixer Specifications

Chamber Bore Diameter	1.547 in
Chamber Bore Length	1.875 in
Capacity Without Blades	1.25 cm^2
Capacity With Blades	69 cm^2
Speed Ratio	3:2
Roller Blade Diameter	1.435 in
Bore to Rotor Clearance	0.056 in
Displacement Volume	56 cm^2

All of the blends were processed under the same conditions. The processing temperature for the blends was 200° C, which is on the lower end of the processing window for both the PS and SMA materials. This temperature was selected due to the thermal instability of the HBP above 200° C based on thermogravimetric analysis (TGA). TGA was performed (Figure 15) on a TA Instruments High-Res TGA 2950 at 5° C/min from 25° C to 450° C. The onset of degradation for the HBP was determined to be approximately 250° C.

The blends were prepared by first melting the PS or SMA in the mixer before adding the HBP. Once the HBP was added to the molten base polymer, the two materials were blended for 15 min to ensure a proper degree of mixing and sufficient time for reaction. The processing speed was 55 rpm, which correlates to a shear rate in the range of 42 s^{-1}–63 s^{-1} [82].

2.4 Post-Processing Rheology - Parallel Plate Viscometer. Rheological studies were carried out according to ASTM Standard D4440-95 after blending in order to determine any change in the processing characteristics of the polymer blends as a result of the addition of HBP. In a dynamic mechanical test, an oscillatory strain is applied to the material and resulting stresses
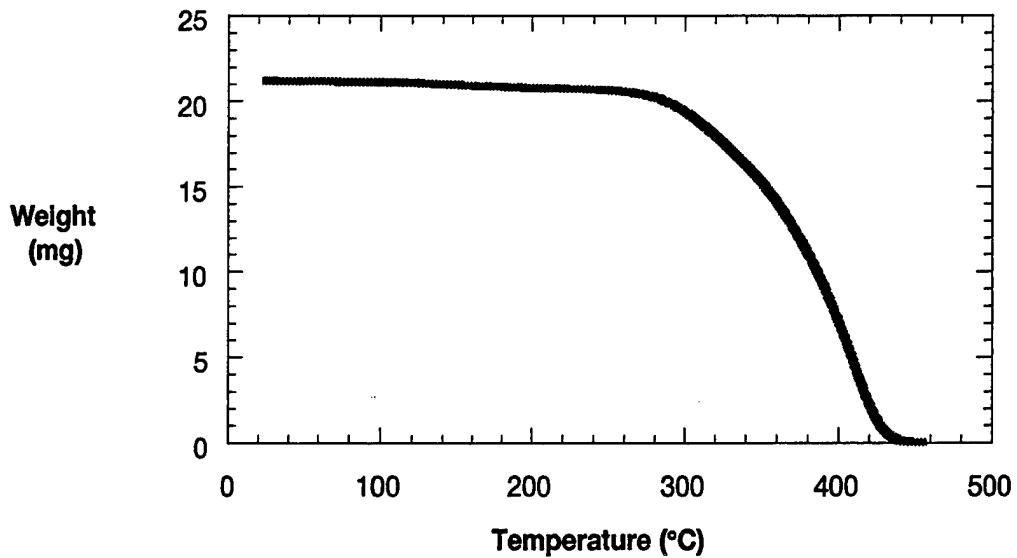
Figure 15. TGA of HBP.

are measured [83]. For an ideal solid that obeys Hooke's law, the resulting stress is proportional to the applied strain amplitude, the stress and strain signals are in phase with one another. For an ideal Newtonian liquid, the stress is proportional to the strain rate. Here, the stress signal is out of phase with the strain signal, leading by 90°.

The stress signal resulting from a viscoelastic polymer can be broken up into two components: an elastic stress that is in phase with the strain and a viscous stress that is in phase with the strain rate, again, 90° out of phase. The elastic stress is a measure of the degree to which a material behaves as an elastic solid. The viscous stress is a measure of the degree to which a material behaves as an ideal fluid. Depending on the test performed, valuable information on polymer viscosity can be collected at several temperatures, shear rates, and frequencies.

A Rheometrics System 4 parallel plate rheometer was used in a frequency sweep mode over a range of 0.01 s^{-1}–100 s^{-1} at 10% strain. The processing temperature of 200° C was used for measurement to simulate actual processing conditions in the Haake Rheomix 600 mixer.

16

2.5 Morphology. As an indication of reaction in the polymer blends, morphological studies were used to examine the second-phase particle segregation in the individual blends. The morphology of the blends will help to determine the compatibility and properties of the polymers [13–14].

Microscopy samples were prepared by freezing the polymer blends in liquid nitrogen for 10 min and impacting them to create fresh fracture surfaces for study. The second-phase material had to be removed to obtain a proper contrast for data analysis. The fracture surface with second-phase particles trapped in the matrix was subsequently submerged in methanol, which acted as a selective solvent and totally dissolved the HBP but did not affect the matrix.

The fracture surface was examined at 500× and 1,000× with an Electroscan 2020 environmental scanning electron microscope. Image analysis techniques were employed in order to determine the average particle size and size distribution.

2.6 Thermal Analysis - Differential Scanning Calorimeter (DSC). In order to determine the T_g of the pure components in the blend and any subsequent shift in the T_g of the blends, thermal analysis was employed. In DSC studies, two aluminum specimen trays of equal mass are used—one is an empty reference tray and the other is filled with polymer. During operation, the empty pan is heated at a constant rate. A temperature difference circuit is used to maintain an equal temperature in both the reference and sample trays by proportioning the power to the heaters. More energy is required to heat the polymer-filled tray due to the additional mass present. When the polymer goes through an endothermic or exothermic transition, the power to the heaters is adjusted to maintain their temperatures and a signal proportional to the power difference is recorded. The area under the resulting curve is a direct measure of the change in enthalpy within the polymer [2, 3].

The pure polymers and the 10% HBP blends were all scanned twice on a TA Instruments DSC 2920 at a rate of 20° C/min over a temperature range from −40° C to 200° C. The DSC cell

17

was purged with ultrahigh purity nitrogen gas at a constant flow rate of 80 cm^2/min to prevent sample degradation.

2.7 Fourier Transform Infrared (FTIR). FTIR is an analytical method used to determine information on molecular vibration [84]. When subjected to excitation radiation in selected spectral regions, typically in the range 4,000 and 200 cm^{-1}, molecules undergo changes in vibrational energy states. A particular structure or functional group in a polymer molecule will absorb infrared (IR) energy in specific bands. The resulting absorption peaks are related to specific molecular motions in that group, such as C-H stretching. From the location and intensity of these peaks, a polymer fingerprint can be obtained based upon the structural groups present.

FTIR studies were performed on all pure polymers and blends on a Perkin Elmer Spectrum 2000 FTIR spectrometer. The samples were prepared by dissolving the polymer blend in THF, applying a few drops of the solution onto a 25-mm × 4-mm potassium bromide crystal, and drying in a vacuum oven at 50° C for 10 min. Data from an average of 16 scans over a range of 4,000 cm^{-1} to 400 cm^{-1} at a resolution of 2 cm^{-1} were analyzed using the Perkin Elmer Spectrum v2.0 software.

2.8 Mechanical Testing. In order to determine any change in the impact properties of the PS/HBP and SMA/HBP blends, notched Izod impact tests were performed at room temperature. All materials were conditioned in accordance with ASTM Standard D618-96. A TMI Model 43-1 Impact Tester fitted with a 2 ft-lb hammer was used in accordance with ASTM Standards D256-93a and D5941-96.

2.9 Dynamic Mechanical Analysis (DMA). DMA studies were performed to determine any change in modulus or a shift in T_g. A TA Instruments DMA 2980 was used to measure any change in the storage modulus (E$'$) or loss modulus (E$''$) which may be an indication of reaction taking place in the blends. A shift in the maximum peak of E$''$ corresponds to a shift in T_g, which would further verify DSC and morphological results.

18

The specimens were all cut to the same dimensions of 9.6 mm in length, 5.2 mm in width, and 2.3 mm in thickness. All materials were conditioned in accordance with ASTM Standard D618-96. The materials were tested in a single cantilever mode at a frequency of 10 Hz with an amplitude of 1 μm. The heating rate was 10° C/min over a temperature range of −30° C–150° C. All measurements were conducted in accordance with ASTM Standards D4065-95, D4092-96, and E1640-94.

3. Experimental Results and Discussion

3.1 Blending. The blending of these PS and SMA with the HBP was challenging due to the small quantity of the HBP available as well as the melting characteristics of HBP. The HBP has an extremely low melt viscosity compared to that of the PS or SMA and tended to remain segregated in the melt unless an appropriate mixing scheme was implemented.

Due to the small amount of HBP available for study, the first attempt at blending was in a low-capacity experimental CSI Max Mixing extruder. This process was aborted due to poor mixing efficiency, short residence time, and an extremely low output of the instrument.

The second attempt at blending with a Haake Polylab System fitted with a single screw extruder was an improvement due to the higher output of material and precise monitoring of processing parameters. It was observed that, with as little as 2% HBP by weight added, the torque and pressure in the extruder dropped an order of magnitude in all the blends relative to the torque required to process the pure PS or SMA at the same temperature and speed. This indicates a significant reduction in the melt viscosity due to the addition of HBP or the lubrication of the extruder barrel wall due to the migration of the HBP molecules to the surface of the bulk polymer [68]. The mixing efficiency and residence time was not suitable to provide a desired quality product. The HBP tended to lag behind in the extruder barrel, and a variation in the degree of mixing was apparent upon visible inspection of the extrudate. It was obvious that in order for these materials to blend efficiently a more aggressive mixing process had to be implemented.

All the blends were mixed in small batches in the Haake Rheomix 600 mixer driven by a Haake Rheocord 40 System since an aggressive batch mixing process was required. This method of blending provided sufficient time for the material to melt, mechanically break up, and mix. As the HBP polymer is broken up into smaller droplets in the melt, more surface area is exposed, thus improving the probability of reaction between the hydroxyl and the MA functional groups during blending.

3.2 Post-Processing Rheology - Parallel Plate Viscometer. The rheological properties of all blends examined changed dramatically with the addition of the HBP. The rheological behavior of the PS/HBP blend was different from the behavior observed in the SMA/HBP blends.

In the PS/HBP, the viscosity dropped with the addition of as little as 2% HBP by weight and continued to drop as more HBP was added (Figure 16) at all shear rates. It appears that the HBP simply acted as a lubricant or processing aide in the immiscible blend; therefore, the more HBP added, the lower the blend viscosity.
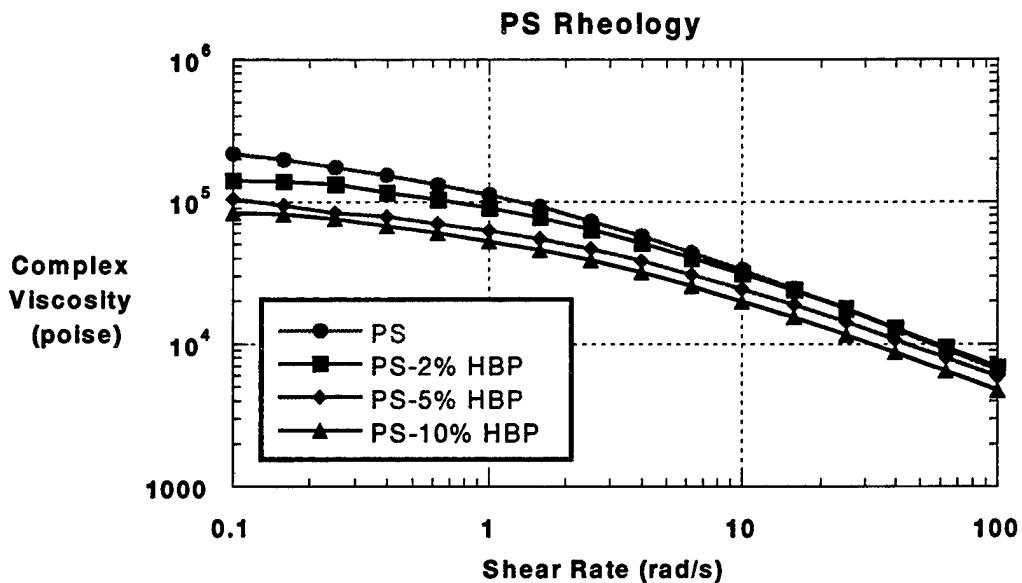

Figure 16. Rheological Behavior of PS With the Addition of HBP.

20

In the SMA/HBP blends, the viscosity dropped with the addition of 2% HBP but did not drop significantly with further addition of HBP (Figures 17 and 18). It appears that there are competing mechanisms taking place. The HBP acts as a processing aide because of its molecular structure and decreases the melt viscosity even though it reacts with the SMA. As more HBP is added, more reactions take place with the SMA, which increase the molecular weight of the newly formed compatibilizers. As the number of reactions increase, the molecular weight increases and the viscosity becomes stabilized at all shear rates.
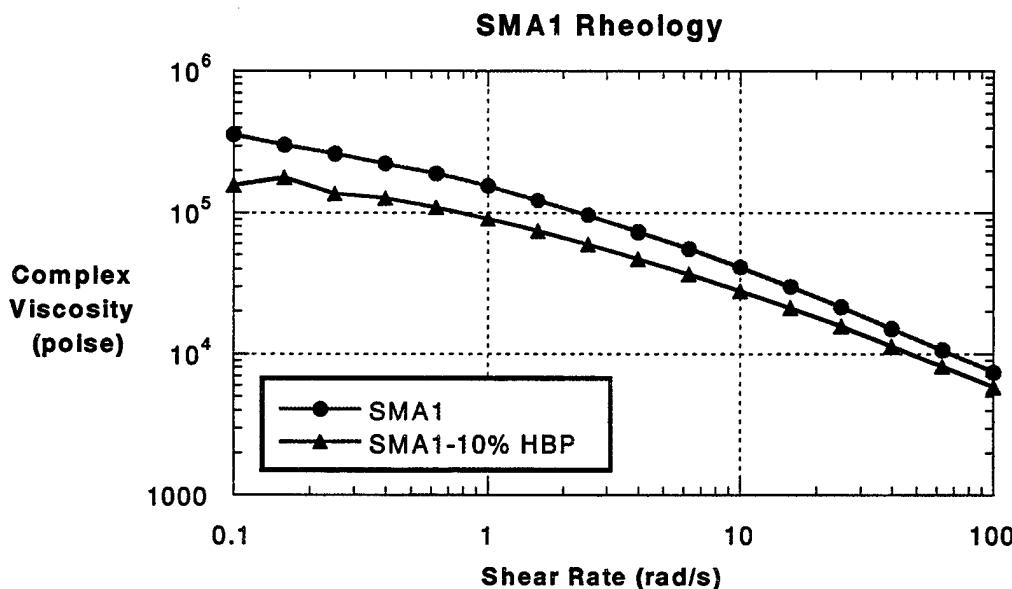
Figure 17. Rheological Behavior of SMA1 With the Addition of HBP.

This rheological behavior is not consistent with most reactive blending schemes whereby there is typically a dramatic increase in the viscosity or torque as reactions take place [11]. This is, however, in agreement with the melt viscosity behavior of hyperbranched molecules and is attributed to the inherent molecular structure of the HBP, which promotes a lower viscosity even at high molecular weights [68]. Once these HBP molecules react with the SMA, the resulting copolymer is a combination of linear and hyperbranched molecules. The structure of these new molecules has a reduced tendency for chain entanglement and promotes a lower viscosity.

21
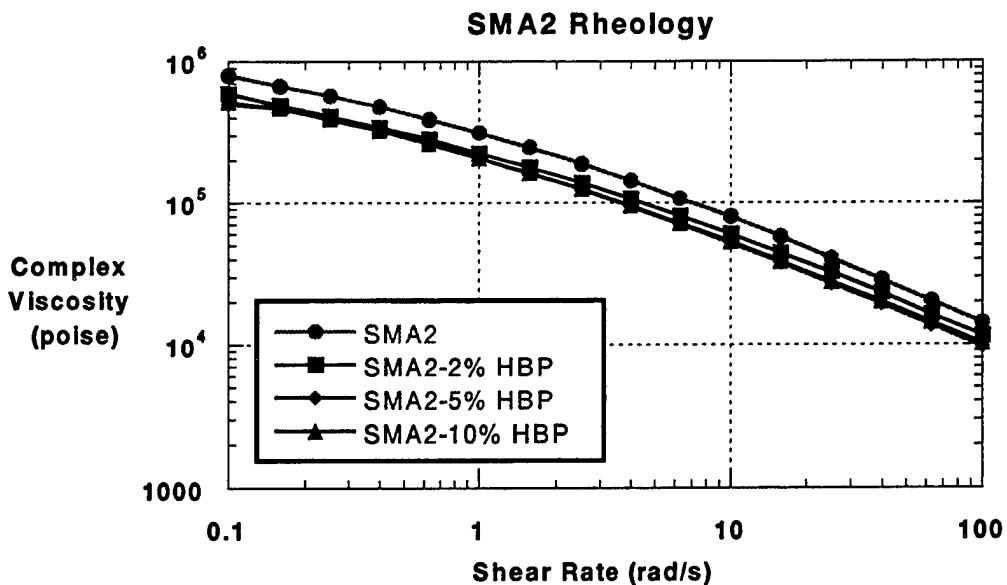
Figure 18. Rheological Behavior of SMA2 With the Addition of HBP.

The rheological data can be plotted at a constant shear rate (Figure 19) to show that there is a different rheological behavior exhibited by the reactive and nonreactive blends. The continuous drop in viscosity of the PS/HBP blend appears to be an additive effect, which results from the increased amount of HBP present. The stabilized viscosity of the SMA/HBP blend, after an initial drop, may be due to the increase in reaction and subsequent increase in molecular weight as the polymers react to form copolymer compatibilizers.

3.3 Morphology. The morphological results from the fracture surfaces of the PS/HBP and the SMA/HBP blends are consistent with expectations based on past research in the area reactive polymer blends [76]. The blends are expected to fall into one of two categories of polymer blends, immiscible or compatibilized. The PS/HBP system is expected to form an immiscible blend whereby two distinct pure phases will be present with a coarse microstructure and large second-phase particles. The SMA/HBP blends are expected to form a compatibilized blend with a refined microstructure and small dispersed second-phase particles.

22

Rheological Behavior of Reactive and Nonreactive Blends

Complex Viscosity (poise)

Shear Rate 66 sec^{-1}

SMA2 Blend

PS Blend

Concentration of HBP (% wt)
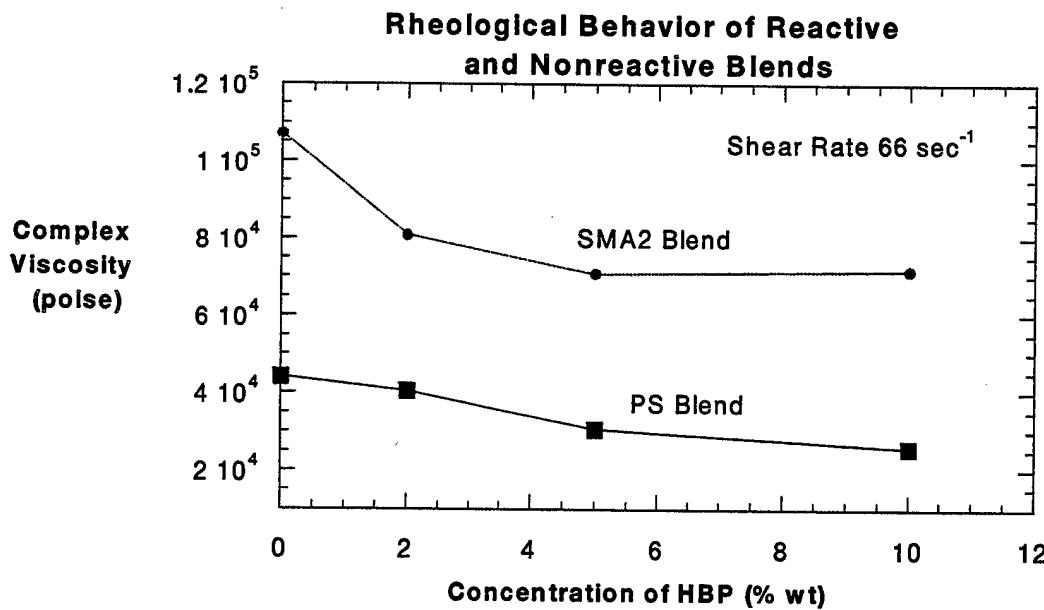
Figure 19. Change in Viscosity at Constant Shear Rate.

The PS/10% HBP blends (Figure 20) exhibit a coarse microstructure with large second-phase particles in an immiscible blend. The average particle size of the PS/HBP blend (Figure 21) is greater than 7.70 µm in diameter. Large HBP particles remain phase separated in a PS matrix at equilibrium due to the lack of reactivity in the system. Coalescence of the HBP phase may also be taking place as the blend cools after processing. This type of morphology is not likely to improve the mechanical properties of the PS homopolymer due to the large particle size and lack of compatibilization at the polymer/polymer interface [5, 13, 14].

The fracture surface of the SMA1/10% HBP blend (Figure 22) has a smaller average particle size when compared to the PS/HBP blend. This observed decrease in particle size in the SMA blend at equilibrium is attributed to a reduction of the interfacial tension and to a restriction in the coalescence mechanisms [85–87], both of which result from the formation of a copolymer or compatibilizer during processing. The average particle size (Figure 23) is approximately 1 µm and may not be an optimum size for improving the toughness of the blend [88, 89].
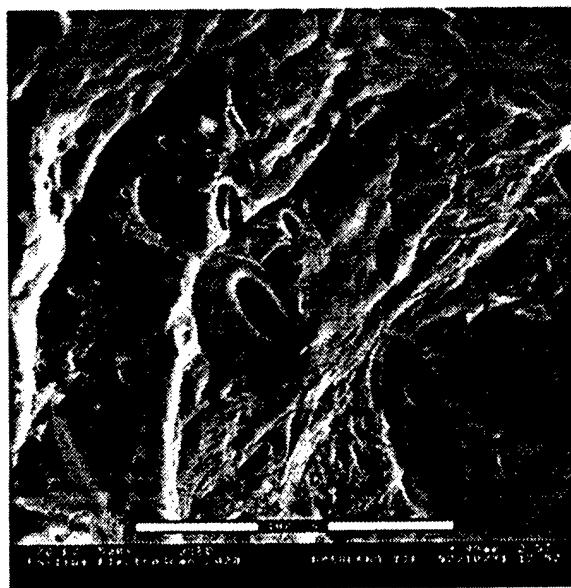
Figure 20. PS/10% HBP Blend Fracture Surface.
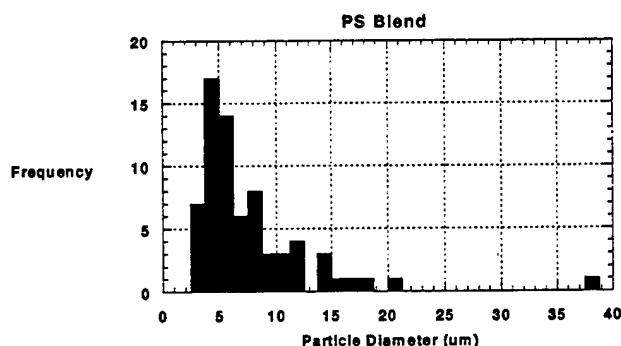
Figure 21. PS/10% HBP Blend Particle-Size Distribution.

The morphology of the SMA2/10% HBP blend (Figure 24) also shows the average particle size (Figure 25) to be on the order of 1 μm and may not be of a proper size to improve the toughness of the blend relative to the pure matrix material [89]. This reduction in average particle size and refinement of the microstructure relative to the PS/HBP blend is due to the formation of compatibilizers during processing.

There is clearly a difference between the second-phase particle size (Table 4) in the SMA/HBP and the PS/HBP blends. It appears that there is no compatibilization in the PS/HBP

24
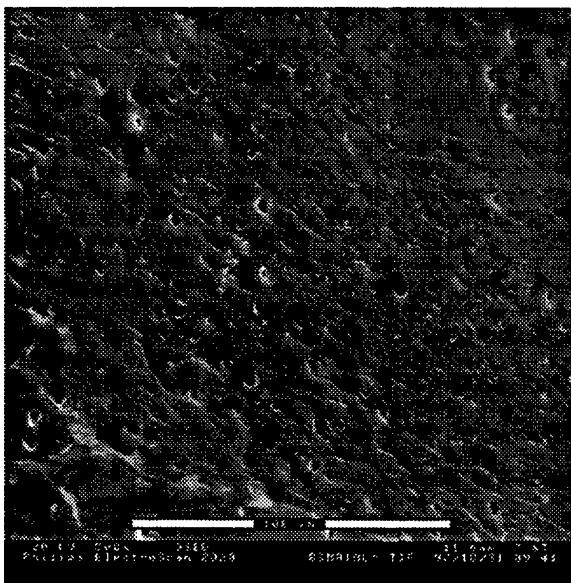
Figure 22. SMA1/10% HBP Blend Fracture Surface.
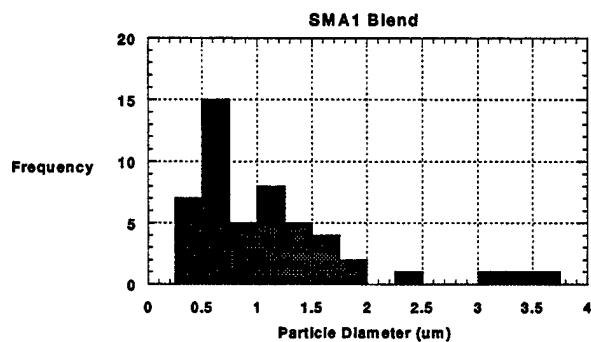
Figure 23. SMA1/10% HBP Blend Particle-Size Distribution.

blend but the SMA/HBP blends appear to be compatibilized due to the observed difference in the microstructure and second-phase particle size at equilibrium.

The microscopy results indicate changes in morphology between the PS-, SMA1-, and SMA2-based blends. However before the observed differences can be attributed directly to compatibilization effects, one must consider the potential effects of differences in viscoelastic properties of the PS, SMA1, and SMA2 matrices on the blend morphology. Predictions from the Taylor Theory are used to assess these effects.
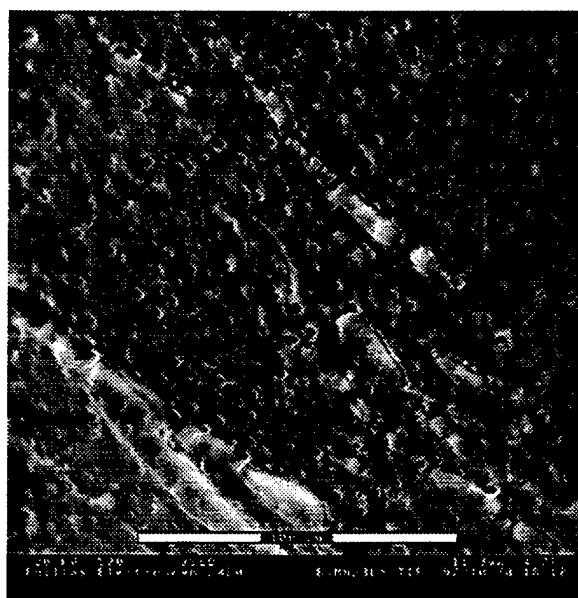
Figure 24. SMA2/10% HBP Blend Fracture Surface.
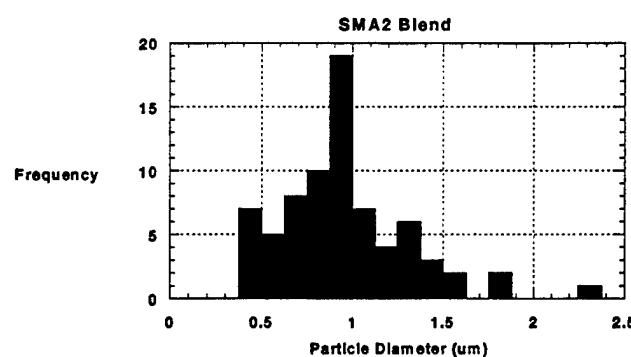
Figure 25. SMA2/10% HBP Blend Particle-Size Distribution.

Table 4. Second-Phase Particle Size

	SMA1	SMA2	PS
Average Diameter (m × 10⁻⁶)	1.1	1.0	7.7
Standard Deviation (m × 10⁻⁶)	0.7	0.4	5.3
Population	50	74	70
95% Confidence Interval	0.2	0.1	1.3

The expected size of the second-phase particles in a two-phase immiscible system can be estimated by the Taylor Equation [90]

$$d = (\gamma_{AB}/G\eta_m)\,(16\lambda + 16/19\lambda + 16), \qquad (2)$$

where d is the particle diameter, γ_{AB} is the interfacial tension between the polymers, G is the shear rate, and λ is the ratio between the dispersed-phase viscosity and the matrix-phase viscosity, η_d/η_m. This theory was originally developed for Newtonian droplets dispersed in a Newtonian fluid under steady shear flow and cannot be directly applied to polymer melts. However, it is considered to be an acceptable starting point for most modern work on droplet dispersion and coalescence [8, 76, 91].

Based on the predictions (Table 5) from the Taylor equation, there would be a difference in the expected particle size for different blends assuming the interfacial tension is constant between the phases in all blends. This size difference in d/d_{ps} is then due to the difference in the melt viscosity between the PS and SMA materials. SMA2 has the highest melt viscosity and the PS has the lowest melt viscosity of the three matrix materials. The second-phase particles in the PS blend should be the largest, the second-phase particles in the SMA1 blend should be smaller, and the second-phase particles in the SMA2 blend should be the smallest.

Table 5. Predicted Relative Size of Second-Phase Particles

Materials	G (s^{-1})	η_m (poise)	η_d (poise)	λ	d/λ_{AB}	d/d_{ps}
PS	66	9200	600	0.065	1.63E-06	1.00
SMA1	66	10700	600	0.056	1.40E-06	0.86
SMA2	66	20390	600	0.029	7.39E-07	0.45

The average particle size present is a function of reactivity of the blend. The second-phase particles in the PS matrix were the largest of the three blends at 7.7 μm, and the second-phase particles in both SMA blends were the smaller at approximately 1 μm (Table 4). This is

consistent with the Taylor equation predictions as far as relative particle size. There is, however, an order of magnitude difference in the second-phase particle size between the reactive and nonreactive blends. Based on the Taylor Equation predictions (Table 5), the minor phase particle in the PS blend should be approximately the same size as the minor-phase particle in the SMA1 blend and, at most, twice that of the minor-phase particle diameter in the SMA2 blend. The micrographs show that they are at least 7.7 times the diameter.

This reduction in particle size in the SMA blends is in agreement with research in the area of compatibilized/immiscible blends. This indicates the formation of compatibilizers from the reaction between SMA and HBP, which was confirmed with subsequent FTIR studies. The presence of compatibilizers lowers the interfacial tension between the phases, reduces the inclination for coalescence, and allows refinement of the microstructure [76].

3.4 Thermal Analysis - DSC. DSC is used to determine primary and secondary-phase transitions in polymers and polymer blends by measuring the quantity of heat absorbed or evolved. It is well established that the measurement of T_g in polymers can be used to determine the miscibility and immiscibility of polymer blends [6, 7]. DSC was performed on all of the individual polymers and polymer blends as a confirmation of reaction by determining the T_g and any subsequent shift as a result of compatibilization.

All of the blends under study had two distinct T_g's, each of which is associated with the individual blend components (Tables 6 and 7). The presence of the two distinct T_g's coupled with the microscopy investigations confirm that the blends are not miscible but are in fact either immiscible or compatibilized polymer blends.

Table 6. T_g **Values of Pure Components**

	HBP	PS	SMA1	SMA2
T_g (°C)	32.0	109.0	124.0	135.0

Table 7. T_g Values of Blends

PS-10	T_g (°C)	SMA1-10	T_g (°C)	SMA2-10	T_g (°C)
HBP Phase	31.1	HBP Phase	37.2	HBP Phase	41.6
PS Phase	112.2	SMA1 Phase	122.5	SMA2 Phase	136.3

In the present study, the PS/HBP blend showed a behavior typical of an immiscible uncompatibilized blend where no significant shift was observed in either T_g. The lack of shift in T_g (Table 7, Figure 26) is an indication of the incompatibility between the blend components.

In both reactive blends, thermal analysis results confirm some degree of compatibilization. A convergent shift of the T_g's is common in compatibilized blends. The T_g associated with the SMA component did not shift significantly in either SMA/HBP blend; this indicates the presence of an essentially pure SMA phase in the blend. However, the T_g associated with the HBP component exhibited a positive shift toward the T_g of the SMA component. A positive shift of the second-phase T_g is an indication of reaction and the incorporation of SMA in the HBP second phase. The second phase now appears to be an intimate mixture of HBP and SMA while the primary phase is essentially pure SMA.

The size of this T_g shift increased with an increase in the MA functional groups present in the SMA matrix (Table 7). The SMA1/HBP (Figure 27) blend resulted in a moderate T_g shift of about 5.2° C. The higher reactivity SMA2 blended with the HBP (Figure 28) resulted in a larger T_g shift of 9.6° C.

As mentioned, an increase in the T_g of the HBP phase can be attributed to the incorporation of SMA molecules into this second phase. The size of the shift in T_g is due to both the amount of SMA incorporated into the second phase as well as the T_g of the SMA incorporated into the second phase. If we consider the HBP phase to be a miscible blend or an intimate mixture of compatibilized SMA and HBP, we can use analysis based on the Fox equation to estimate the amount of SMA incorporated into the HBP phase.

PS DSC
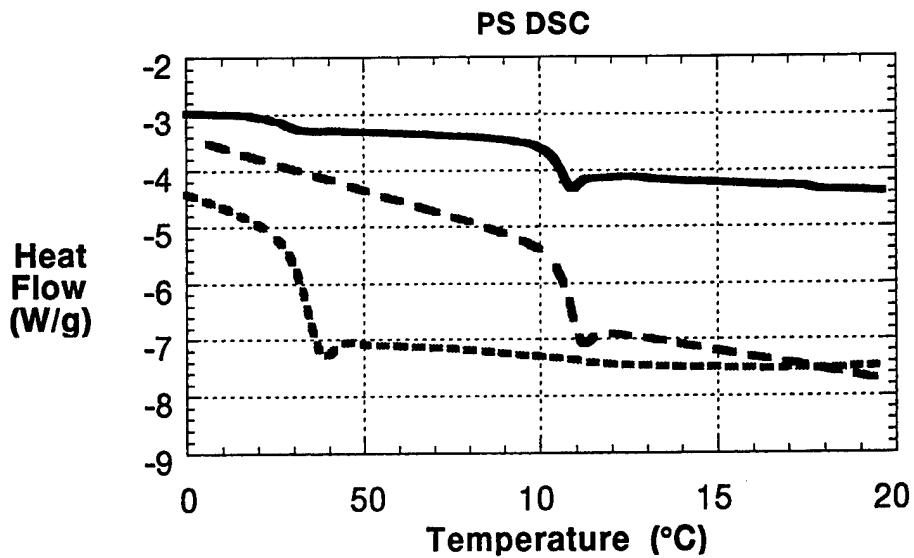
Figure 26. DSC Curves: PS Blend (Top), PS (Middle), and HBP (Bottom).

SMA1 DSC
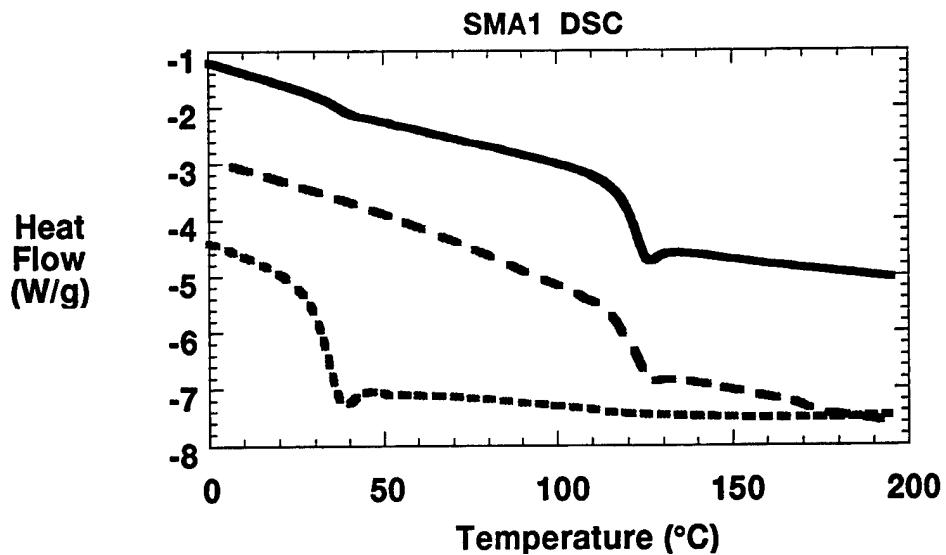
Figure 27. DSC Curves: SMA1 Blend (Top), SMA1 (Middle), and HBP (Bottom).

In a miscible blend, a single T_g is typically observed in between the T_g's of the individual components [6]. The position of the blend T_g (T_{gb}) can be determined using the Fox equation and is related by mass fraction ($m_{1,2}$) and $T_{g1,2}$ of the individual components [2, 3].

30
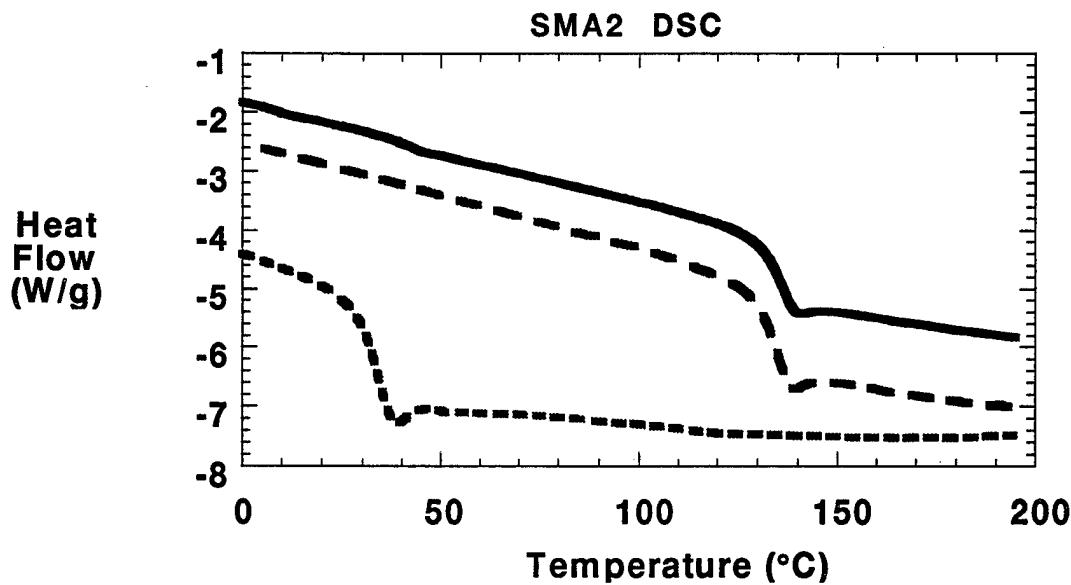
Figure 28. DSC Curves: SMA2 Blend (Top), SMA2 (Middle), and HBP (Bottom).

$$1/T_{gb} = m_1/T_{g1} + m_2/T_{g2}. \tag{3}$$

In an immiscible blend, two discrete T_g's should be observed, since no reaction or compatibilization takes place and the two phases are essentially pure. Each peak is associated with the T_g of the individual components. The T_g's observed will be the same as the T_g's for the individual components. The intensity of the peak observed for each T_g depends on the amount of each component present in the blend.

In a compatibilized blend, two discrete T_g's should be observed. Each peak is also associated with the T_g of the individual components. Since reactions are taking place and compatibilizers are formed that become intimately mixed with the pure phases at the interface, the two phases are no longer pure. The T_g's observed might not be the same as the T_g's for the individual components but rather shift and converge on each other. This convergence indicates reaction and compatibilization.

31

A positive 5.2° C shift in T_g is consistent with the incorporation of 6% SMA1 by weight in the HBP phase. Similarly, a positive 9.6° C shift in T_g is consistent with the incorporation of 11% SMA2 by weight into the HBP phase (Table 8, Figure 29, equation [3]).

Table 8. Fox Equation Estimation of Amount of SMA Present in HBP Phase

DSC Data	T_g HBP Phase (K)	Mass Fraction HBP	T_g HBP (K)	Mass Fraction SMA	T_g SMA (K)
SMA1	310.50	0.94	305.00	0.06	396.00
SMA2	314.00	0.89	305.00	0.11	408.00
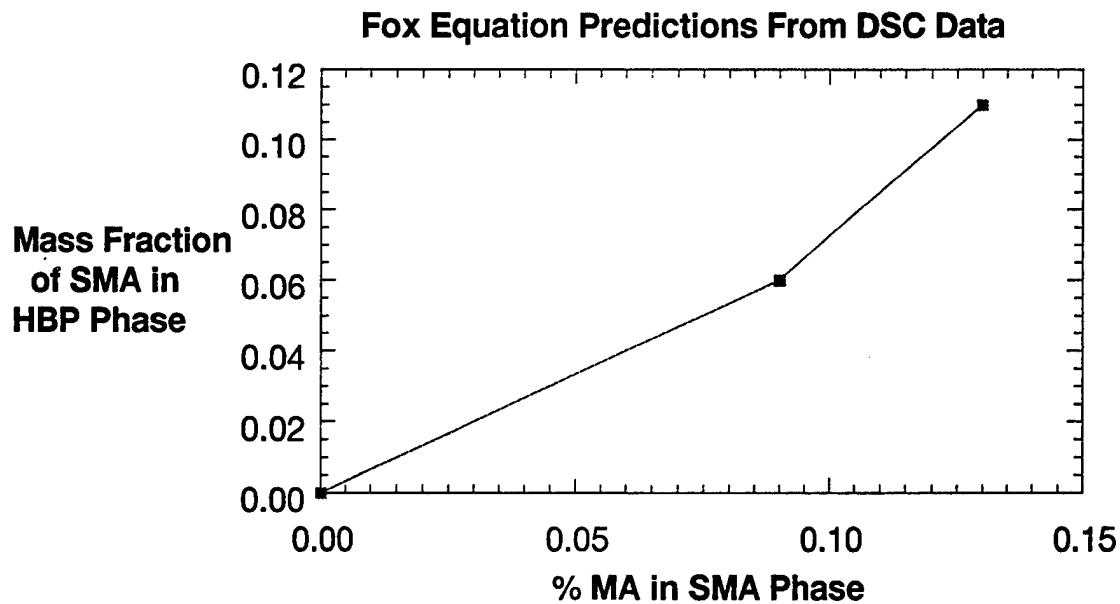
Figure 29. Fox Equation Prediction of Amount of SMA Present in HBP Phase.

As expected, the percent of SMA in the HBP phase in the reactive blends increased as a function of increased reactivity in the SMA matrix. This phenomenon implies an increase in compatibility as a function of increased matrix reactivity. As the compatibility between the two phases increases, an improvement in mechanical properties may result due to improved interfacial adhesion and a refined morphology.

3.5 FTIR. FTIR was used in order to confirm reaction in the polymer blends. Scans of the pure materials were taken before blending in order to obtain a baseline. FTIR spectra were taken for the PS/10% HBP and SMA/10% HBP blends processed in the batch mixer. The results suggested reaction but the data fell within the error of the spectrometer and were thus inconclusive.

In order to prove that the SMA and HBP materials react with one another, solution blends were prepared with 50% HBP by weight. The 9:1 ratio of hydroxyl to MA functional groups greatly increased the likelihood of reaction. Equal weights of SMA and HBP were placed in THF and heated to 50° C until they went into solution. The solution was then poured into 100 ml of H_2O, which acted as a nonsolvent, and the polymer precipitated from solution. The now intimate mechanical mixture of polymer was dried and baked at 200° C for 30 min to simulate processing temperatures.

Peaks in the spectra represent different chemical structures in each polymer molecule. Certain peaks are common among several of the resins examined; others are unique to individual polymers.

The benzene ring present in the PS, SMA1, and SMA2 polymers (Figures 30, 31, 32) absorbs strongly at 700 cm^{-1} and 755 cm^{-1}; weaker absorption peaks are present at 1,452 cm^{-1} and 1,493 cm^{-1}, respectively.

The maleic anhydride ring present in the SMA1 and SMA2 resins (Figures 31 and 32) absorbs strongly at 1,781 cm^{-1}. This peak is expected to decrease as the rings open and react with the hydroxyl functional groups on the HBP.

The HBP polymers absorb strongly at 1,732 cm^{-1} due to the large number of carbonyl groups present (Figure 33). As the –OH functional end groups react with the MA, the ring structure breaks open and covalent bonds are formed; the size of this peak should increase in the reactive

PS - FTIR
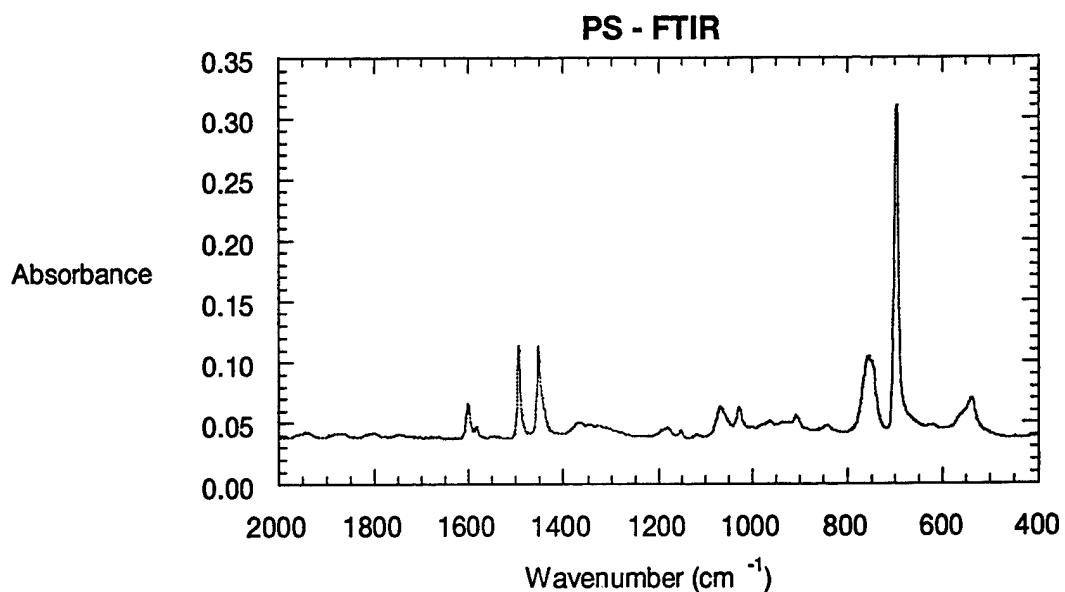
Figure 30. FTIR Spectra of Polystyrene.

SMA 1 - FTIR
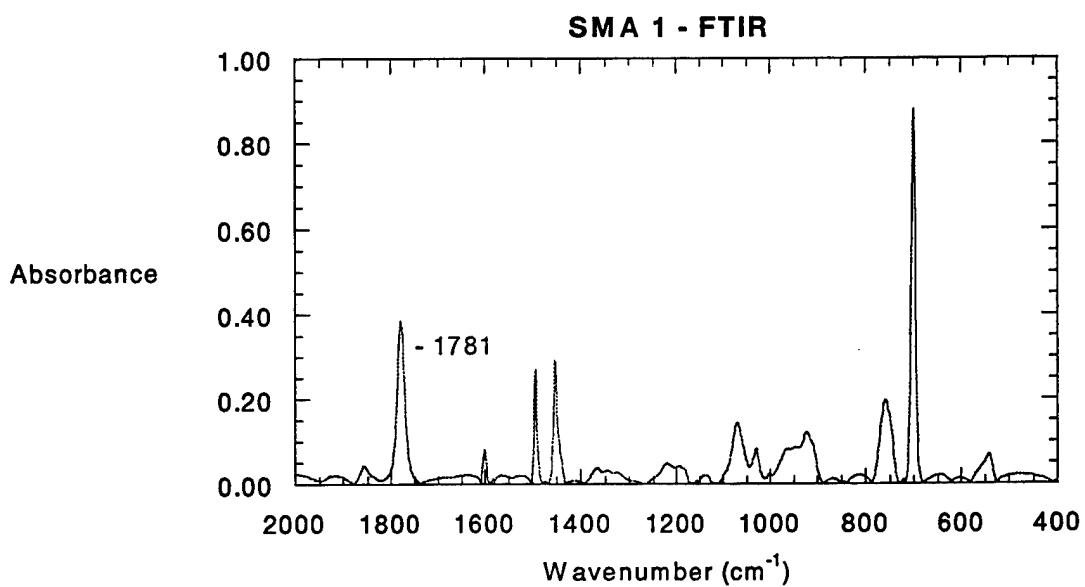
Figure 31. FTIR Spectra of Styrene Maleic Anhydride 1.

blend spectra. This is due to an increase in the number of conjugated ester groups formed as the two materials react.

SMA2 - FTIR
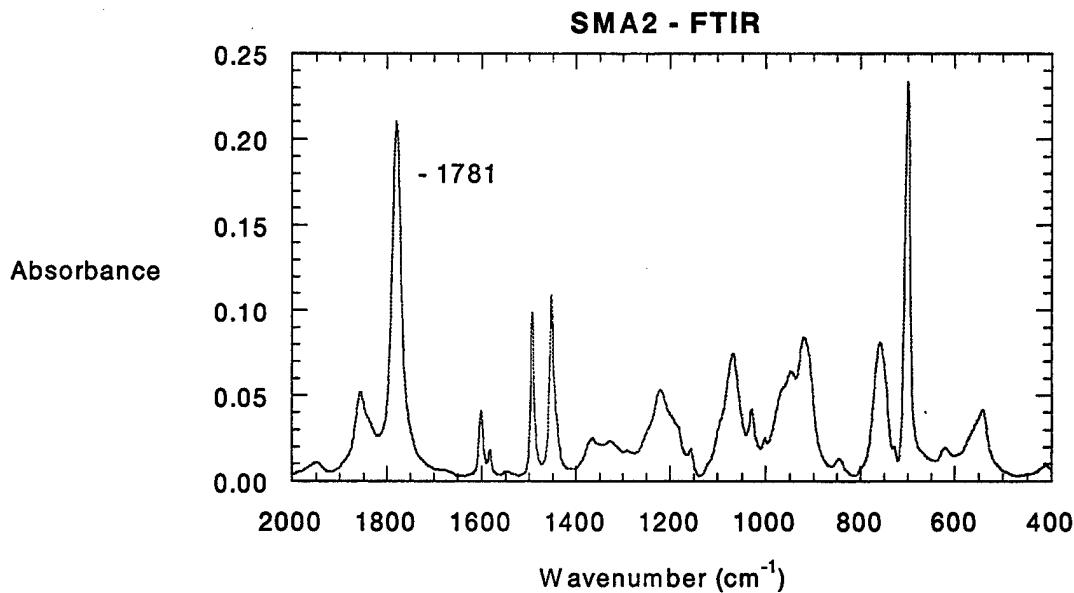
Figure 32. FTIR Spectra of Styrene Maleic Anhydride 2.

HBP - FTIR
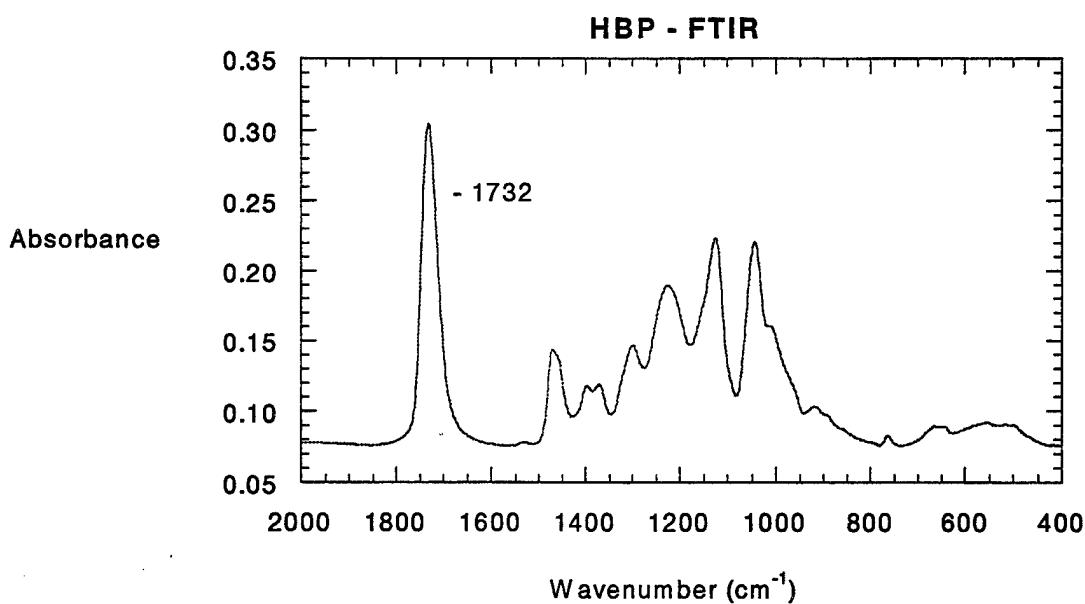
Figure 33. FTIR Spectra of Hyperbranched Polyol.

In a typical immiscible, uncompatibilized blend, all of the peaks from the two pure polymers will be present in the blend. This is the case for the PS/HBP blend (Figure 34), where there is no evidence of a band shift in any region. There are not any new peaks present nor have any of the

35

PS - FTIR
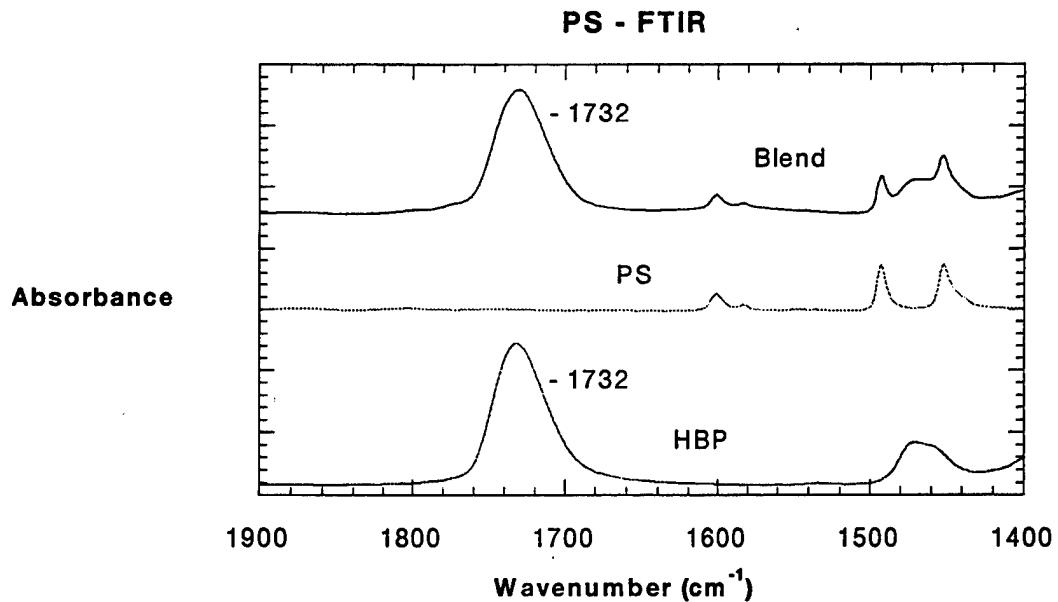
Figure 34. FTIR Spectra of Polystyrene Blend.

baseline peaks disappeared. The spectra of the nonreactive blend are essentially a combination of the PS spectra and the HBP spectra.

This is not the case in the FTIR spectra from the two reactive blends examined. In a reactive blend, the functional group chemical structure will change as it reacts with other reactive groups. New peaks may result from the new structural groups created in the blend during processing. The absence of specific peaks in the blend that were present in the pure components may also confirm reaction. The absence of a peak at $1,781 \text{ cm}^{-1}$ in the SMA1 and SMA2 blends (Figures 35 and 36) signifies a depletion of MA rings in the system and proves that the ring opening reaction between MA and –OH may take place in the system at processing temperatures.

3.6 Mechanical Testing. The pure PS and SMA materials have poor impact properties due to their inability to absorb energy via crazing or shear yielding mechanisms. During impact, a sharp crack is initiated and continues to propagate freely until fracture occurs in a brittle fashion. The addition of a rubbery second phase with a low T_g has been proven to improve the impact

36

SMA1 - FTIR
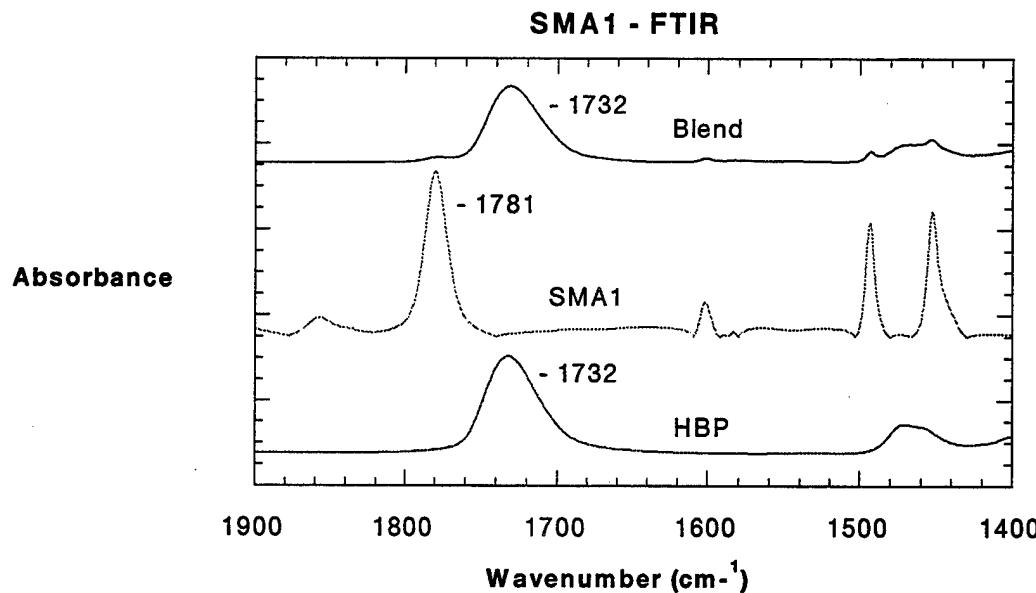
Figure 35. FTIR Spectra of SMA1 Blend.

SMA2 - FTIR
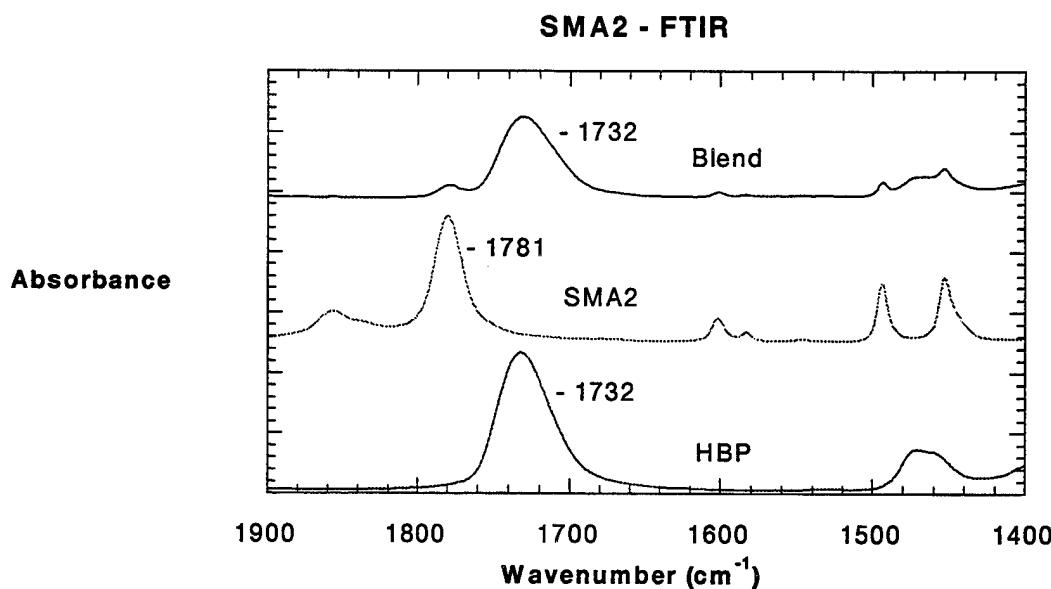
Figure 36. FTIR Spectra of SMA2 Blend.

properties of a glassy material [16]. In blending HBP with PS and SMA, an improvement in the impact properties of the blends when compared to those of pure material was desired.

37

In this study, the impact properties of the blends did not improve. In both the SMA/HBP and PS/HBP blends (Figure 37, Table 9), a drop in the notched Izod impact strength was observed despite the improvement of the morphology in the SMA/HBP blends. This may be due to several factors. The T_g of the HBP is close to room temperature and typically the addition of a toughener with low T_g is desirable for an improvement in impact properties. Another possible explanation for the decrease in impact strength may be that the second-phase particles are not an optimum size for this particular system [88].

Notched Izod Impact
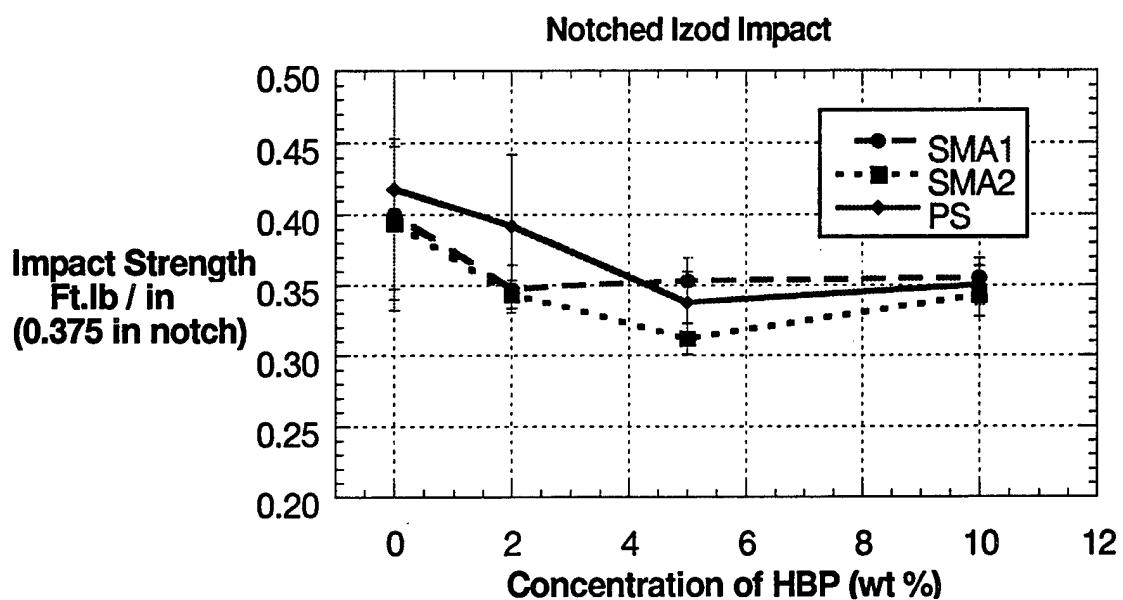
Figure 37. Notched Izod Strength With Addition of HBP.

Table 9. Impact Properties of PS/HBP Blends and SMA/HBP Blends

HPB (%)	SMA1 (ft.lb/in)	Standard Dev	SMA2 (ft.lb/in)	Standard Dev	PS (ft.lb/in)	Standard Dev
0	0.400	0.053	0.394	0.054	0.418	0.086
2	0.347	0.017	0.344	0.010	0.392	0.050
5	0.354	0.016	0.312	0.011	0.338	0.022
10	0.355	0.014	0.343	0.015	0.350	0.014

The impact properties of a brittle resin are generally improved by the addition of rubbery particles. The determination of the optimum size is unclear at best and must be resolved for each blend system. The effectiveness of this toughening mechanism depends on the diameter and concentration of these particles as well as the inherent matrix properties [16].

3.7 DMA. In a DMA study of an immiscible polymer blend, two peaks are typically observed in the loss modulus; each peak represents the T_g of a phase, which consists primarily of the individual components [2, 92, 93]. The DMA data for the PS and PS/10% HBP blends (Figure 38) appear to be consistent with the results expected from an immiscible blend. The solid lines represent the PS, and the dashed lines represent the PS/10% HBP blend. The loss modulus of the blend exhibits two distinct T_g's, each located at the same temperature of the pure component. This indicates that each phase is made up of essentially pure material and no compatibilization has occurred.
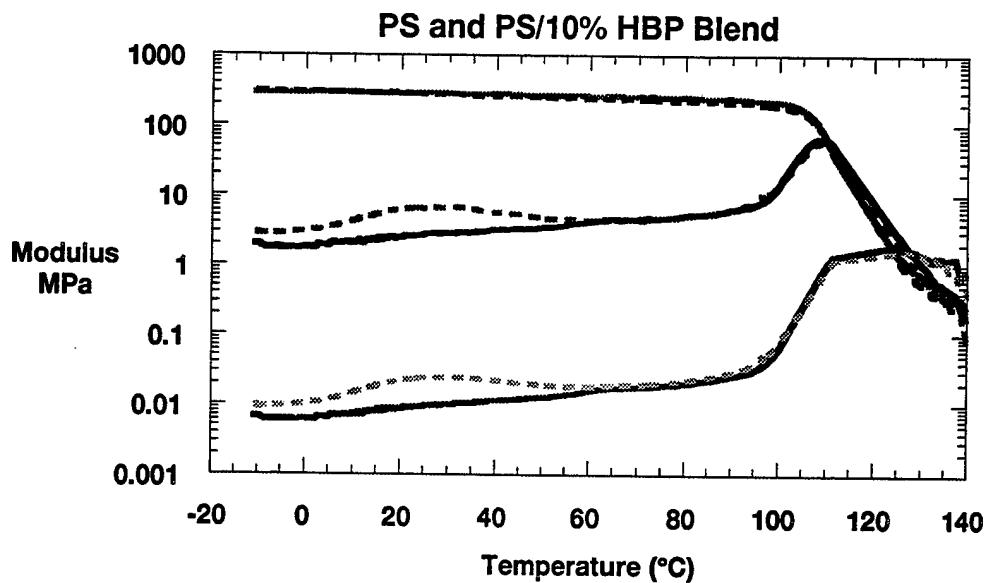

Figure 38. DMA of PS and PS/10% HBP Blend: Top E′, Middle E″, Bottom Tan δ.

In a compatibilized polymer blend, two peaks are typically present in the loss modulus; each peak represents the T_g of a phase, which consists primarily of the individual components. Typically, there will be a convergent shift in one or both of the T_g's associated with the

individual components. The DMA data for the SMA1 and SMA1/10% HBP blends (Figure 39) appear to be consistent with the results expected from a compatibilized blend. The solid lines represent the SMA1, and the dashed lines represent the SMA1/10% HBP blend. The loss modulus of the blend exhibits two distinct T_g's, each associated with the pure components. In the blend, the T_g associated with the SMA1 phase did not shift significantly, but there was a positive shift in the T_g associated with the HBP phase. This indicates that the SMA1 phase is made up of essentially pure SMA1, and the HBP phase is an intimate compatibilized mixture of HBP and SMA1.
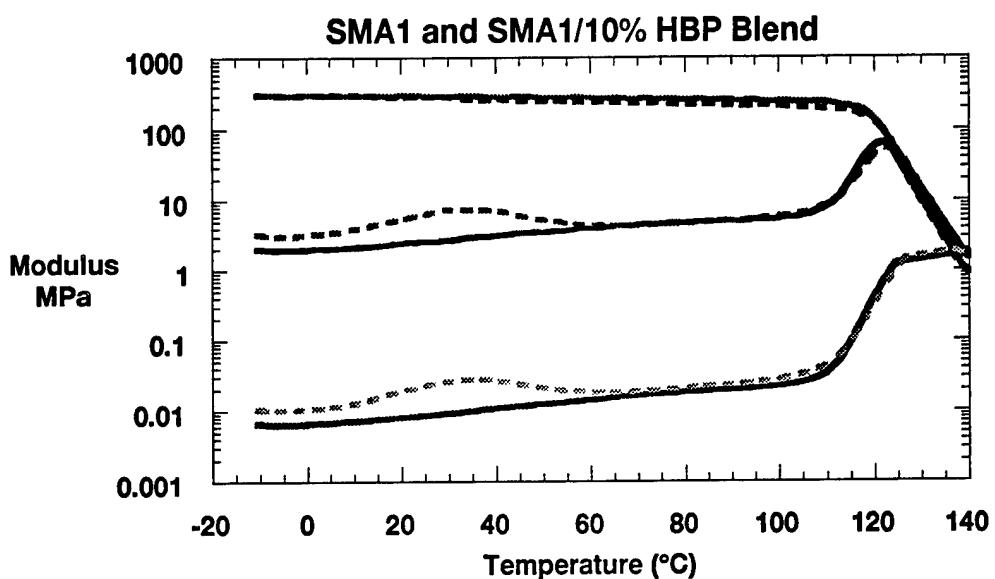
Figure 39. DMA of SMA1 and SMA1/10% HBP Blend: Top E', Middle E'', Bottom Tan δ.

The loss modulus DMA data for the SMA2 and SMA2/10% HBP blends (Figure 40) also appears to be consistent with the results expected from a compatibilized blend. The solid lines represent SMA2, and the dashed lines represent the SMA2/10% HBP blend. The loss modulus of the blend exhibits two distinct T_g's, each associated with the pure components. The T_g associated with the SMA2 phase did not shift significantly, but there was a sizable shift in the T_g associated with the HBP phase. This indicates that the SMA2 phase is made up of essentially pure SMA2 and the HBP phase is an intimate compatibilized mixture of HBP and SMA2.
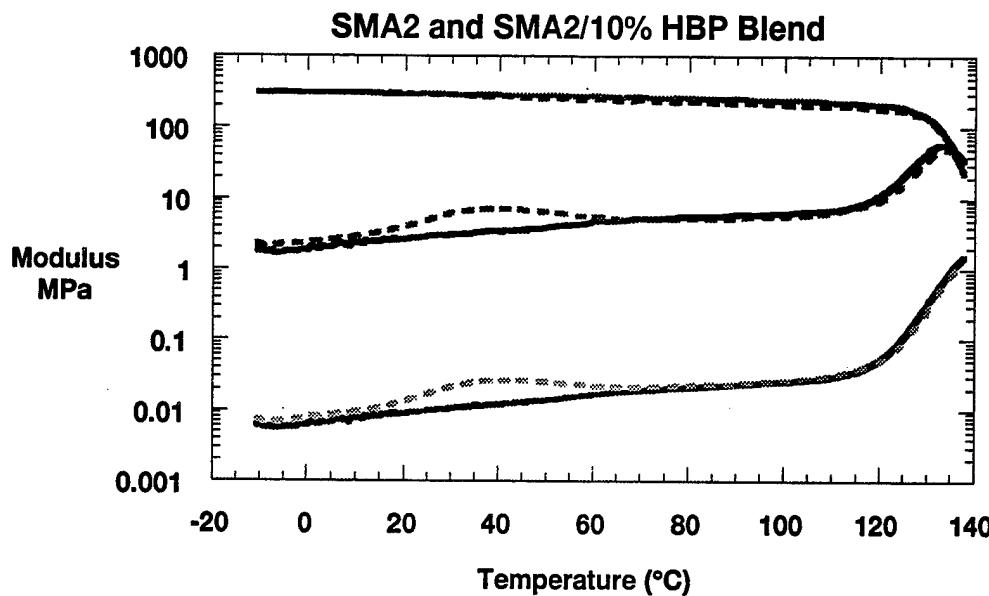
Figure 40. DMA of SMA2 and SMA2/10% HBP Blend: Top E′, Middle E″, Bottom Tan δ.

The DMA results are consistent with the DSC results. The loss modulus peaks associated with the HBP phase in the PS/HBP and SMA/HBP blends exhibited a positive shift in T_g as a function of matrix reactivity (Figures 41 and 42). Although T_g data for blends at low concentrations of HBP could not be determined from DSC analysis, DMA was able to determine information about the T_g of the HBP phase at all concentrations of HBP loading. As observed in the 10% blends, there was no shift in the T_g of the HBP phase for the PS/HBP blends. A small shift in the T_g of the HBP phase for the SMA1/HBP blends and a large shift in the T_g of the HBP phase in the SMA2/HBP blends were observed.

As with the DSC results, the lack of a shift in the second phase T_g of the PS/HBP blend is due to the absence of reactivity in the system. The shift in the Tg of the HBP phase in the HBP/SMA blends can be attributed to the incorporation of SMA into the HBP phase. The relative size of the shift is due to both the amount of SMA incorporated as well as the T_g of the SMA incorporated.

41

Tg Shift of HBP Phase
5% Blend

PS-5
SMA1-5
SMA2-5

Loss Modulus

Tg HBP

Tg

Temperature (°C)
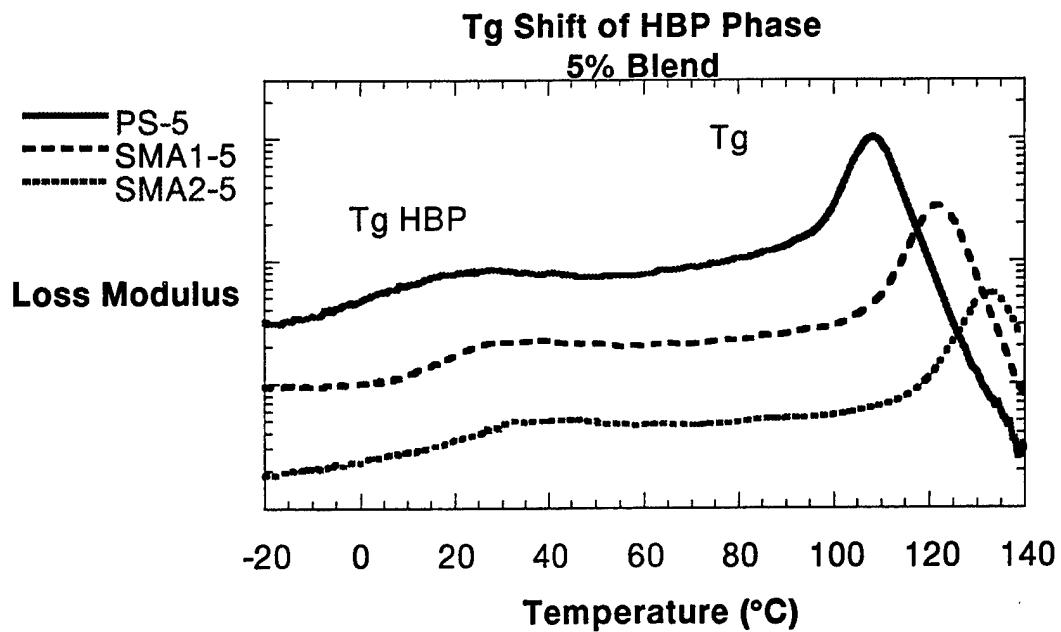
Figure 41. T$_g$ Shift as a Function of System Reactivity: 5% HBP Loading.

Tg Shift of HBP Phase
10% Blend

PS-10
SMA1-10
SMA2-10

Loss Modulus

Tg HBP

Tg

Temperature (°C)
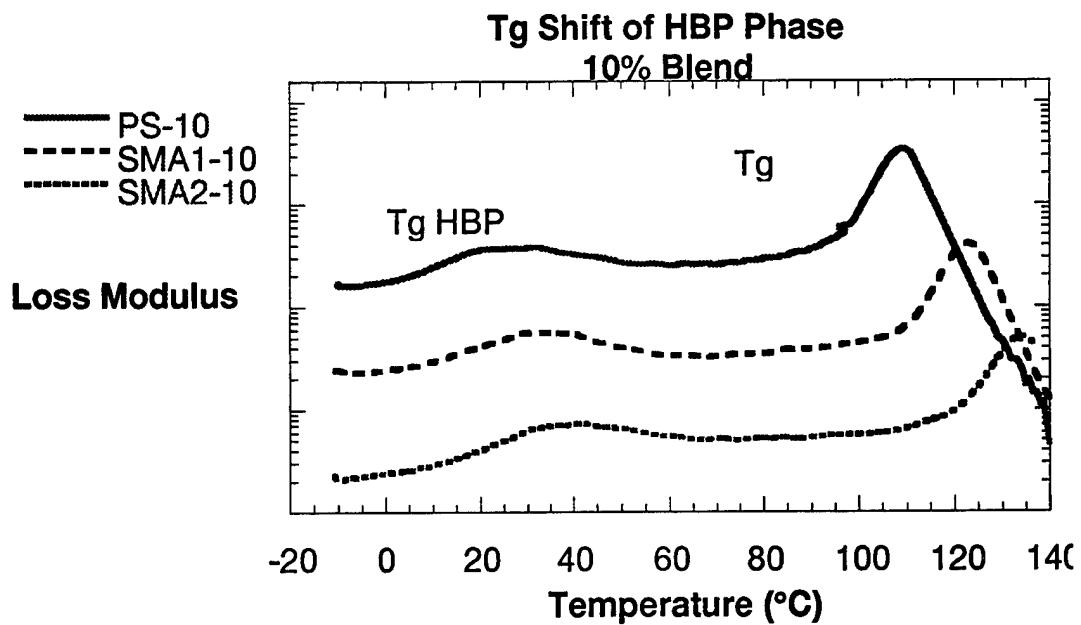
Figure 42. T$_g$ Shift as a Function of System Reactivity: 10% HBP Loading.

This study demonstrated qualitatively the relative shift in the T$_g$ of the HBP phase as a function of matrix reactivity. In addition to the T$_g$ data, DMA showed that there was essentially

42

no change in the storage modulus due to the addition of HBP in both the reactive and nonreactive blends.

4. Conclusions

Hyperbranched polymer molecules are attractive due to their unique highly branched three-dimensional structure and high density of functional endgroups. These factors make them a natural for use as blend modifiers for improved processing characteristics and reactive compatibilization.

The blending of HBP with PS or SMA resulted in an improvement in the processing characteristics of the blends. The post-processing rheological studies illustrated a dramatic decrease in the melt viscosity of both reactive and nonreactive blends. The reactive blend viscosity deceased but stabilized as the loading of HBP increased and as the amount of high molecular weight compatibilizers in the blend increased. The viscosity of the nonreactive blend also decreased as HBP was introduced into the system but continued to drop as more HBP was added.

ESEM studies illustrated an order of magnitude difference in the second-phase particle size of the reactive and nonreactive blends. The reactive blends possess a refined morphology with a small second-phase particle size on the order of a 1 μm in diameter. The nonreactive blends exhibit a coarse morphology with a second-phase particle size in excess of 7 μm in diameter.

The thermal analysis revealed a shift in the T_g of the HBP phase in the reactive blends but no shift in the HBP phase of the nonreactive blend. This shift in T_g is an indication of reaction between the hydroxyl groups on the HBP and the MA groups of the SMA. The size of the shift increases with increasing matrix reactivity and depends on both the T_g of the SMA matrix as well as the amount of SMA incorporated into the HBP phase.

FTIR analytical methods confirmed the reaction resulting in the formation of compatibilizers during processing in the reactive blends. The peak at 1,781 cm^{-1} in the SMA spectra associated with the maleic anhydride ring disappears in the SMA blend spectra as reactions occur with the hydroxyl groups present in the HBP. No such change in the spectra of the nonreactive blends was observed.

The impact properties of the reactive and nonreactive PS were not improved by the addition of HBP. The T_g of the HBP may be too high to demonstrate improved toughening characteristics or the optimum second-phase particle size may not have been achieved during processing.

DMA agrees with the DSC studies and supports the presence of reactively compatibilized blends. The shift in the T_g of the HBP phase increased with increased matrix reactivity. DMA also showed that there was no significant change in the modulus of any blend with the addition of HBP.

Hyperbranched polymers have demonstrated their usefulness in reactive processing schemes. Through a reactive compatibilization scheme, blends were created with improved processing characteristics, a refined morphology with dispersed second-phase particles and the potential for improved mechanical properties.

5. Recommendations

Further research into the behavior of these polymer blends must be performed to better understand the reactions that occur during processing and how they relate to the rheological/ mechanical properties of the blend. Future work includes processing blends with higher volume fractions of HBP to better characterize the rheological behavior as a function of HBP concentration. The blending of different generations of HBP with SMA at different shear rates and temperatures will establish the optimum second-phase particle size and processing variables for a reactively compatibilized blend with improved mechanical properties. Continued research

into processing and practical applications of hyperbranched polymers will demonstrate the ultimate worth of these truly unique polymers in the material science arena.

6. References

1. Utracki, L. A. "History of Commercial Polymer Alloys and Blends." *Polymer Engineering and Science*, vol. 35, no. 1, pp. 2–18, 15 January 1995.

2. Sperling, L. H. *Introduction to Physical Polymer Science*. New York: Wiley and Sons, 1992.

3. Billmeyer, F. W. *Textbook of Polymer Science*. New York: Wiley and Sons, 1984.

4. De Gennes, P. G. "Polymers at an Interface; a Simplified View." *Advances in Colloid and Interface Science*, vol. 27, pp. 189–209, 1987.

5. Wu, S. "Phase Structure and Adhesion in Polymer Blends: A Criterion for Rubber Toughening." *Polymer*, vol. 26, p. 1855, November 1985.

6. Paul, D. R. "Polymer Blends." New York: Academic Press, 1978.

7. Paul, D. R. *Encyclopedia of Polymer Science and Engineering*. New York: Wiley and Sons, vol. 12, p. 399, 1986.

8. Utracki, L. A. "Development of Polymer Blend Morphology During Compounding in a Twin Screw Extruder. Part 1: Droplet Dispersion and Coalescence – a Review." *Polymer Engineering and Science*, vol. 32, p. 1824, 1992.

9. Xanthos, M., and S. S. Dagli. "Compatibilization of Polymer Blends by Reactive Processing." *Polymer Engineering and Science*, vol. 31, no. 13, p. 929, July 1991.

10. Okamoto, M., and T. Inoue. "Reactive Processing of Polymer Blends: Analysis of the Change in Morphological and Interfacial Parameters With Processing." *Polymer Engineering and Science*, vol. 33, no. 3, p. 175, February 1993.

11. Fowler, M. W., and W. E. Baker. "Rubber Toughening of Polystyrene Through Reactive Blending." *Polymer Engineering and Science*, vol. 28, no. 21, p. 1427, November 1988.

12. Brown, S. B. *Encyclopedia of Polymer Science and Engineering*. New York: Wiley and Sons, vol. 14, p. 169, 1986.

13. Scott, C. E., and C. W. Macosko. "Processing and Morphology of Polystyrene/Ethylene Propylene Rubber Reactive and Nonreactive Blends." *Polymer Engineering and Science* vol. 35, no. 24, December 1995.

14. Scott, C. E., and C. W. Macosko. "Morphology Development During Reactive and Nonreactive Blending of an Ethylene Propylene Rubber With Two Thermoplastic Matrices." *Polymer*, vol. 35, no. 25, 1994.

15. Simmons, A. *Polymer Communications*, vol. 31, p. 20, January 1990.

16. Utracki, L. A. "A New Computational Model With Coalescence." *Polymer Engineering and Science*, vol. 35, no. 1, pp. 115–128, 15 January 1995.

17. Liu, N. C., and W. E. Baker. "Reactive Polymers for Blend Compatibilization." *Advances in Polymer Technology*, vol. 11, no. 4, pp. 249–262, 1992.

18. Willis, J. M., and B. D. Favis. "Reactive Processing of Polystyrene-co-Maleic Anhydride/ Elastomer Blends: Processing Morphology Property Relationships." *Polymer Engineering and Science*, vol. 30, no. 17, p. 1073, 1990.

19. Stinson, S. "Reactive Processing of Plastics Yields Improved Polymers." *C&EN*, p. 20, 15 January 1996.

20. Beck Tan, N. C. "Reactive Reinforcement of Polystyrene/Poly (2-vinylpyridine) Interfaces." *Macromolecules*, vol. 29, no. 14, pp. 4969–4975, 1996.

21. Tomalia, D. A. "Dendrimer Molecules." *Scientific American*, p. 62, May 1995.

22. Flory, P. J. "Molecular Size Distribution in Three-Dimensional Polymers." *Journal of American Chemical Society*, vol. 74, 1953.

23. Tomalia, D. A. "Dendritic Macromolecules: A Fourth Major Class of Macromolecular Architecture." *PSME*, vol. 73, Fall 1995.

24. Tomalia, D. A. U.S. Patent 4435548, 1984.

25. Tomalia, D. A. U.S. Patent 5773527, 1998.

26. Hedstrand, D. M. U.S. Patent 5393797, 1997.

27. Frechet, J. T. U.S. Patent 5041516, 1997.

28. Hedstrand, D. M. U.S. Patent 5387617. 1998.

29. Newkome, G. R. U.S. Patent 5773551. 1998.

30. Matyjaszewski, K. U.S. Patent 5763548, 1998.

31. Mager, M. U.S. Patent 5679755, 1998.

32. Juneau, K. N. U.S. Patent 5777129, 1998.

33. Newkome, G. R. U.S. Patent 5422379, 1998.

34. Swanson, D. R. U.S. Patent 5705573, 1998.

35. Turner, S. R. U.S. Patent 5196502, 1998.

36. Klee, J. E. U.S. Patent 5760142, 1998.

37. Wright, D. C. U.S. Patent 5795582, 1997.

38. Jansen, J. F. U.S. Patent 5788989, 1997.

39. Hansen, H. J. U.S. Patent 5635603, 1997.

40. Urdea, M. S. U.S. Patent 5594118, 1998.

41. Virtanen, J. U.S. Patent 5718915, 1998.

42. Tezon, J. G. U.S. Patent 5736346, 1998.

43. Platzek, J. U.S. Patent 56501364, 1998.

44. Platzek, J. U.S. Patent 5759518, 1998.

45. Keefer, L. K. U.S. Patent 5676963, 1998.

46. Szoka, F. C. U.S. Patent 5661025, 1997.

47. Keefer, L. K. U.S. Patent 5650447, 1997.

48. Keefer, L. K. U.S. Patent 5405919, 1995.

49. Tomalia, D. A. U.S. Patent 5714166, 1998.

50. Mead, S. B. U.S. Patent 5596027, 1997.

51. Winnik, F. M. U.S. Patent 5256516, 1998.

52. Breton, M. P. U.S. Patent 5266106, 1998.

53. Winnik, F. M. U.S. Patent 5098475, 1998.

54. Milco, L. A. U.S. Patent 5731095, 1998.

55. Bahary, W. S. U.S. Patent 5658574, 1998.

56. Gundlach, K. B. U.S. Patent 5254159, 1997.

57. Hedstrand, D. M. U.S. Patent 5560929, 1998.

58. Daroux, M. L. U.S. Patent 5648186, 1997.

59. Tomalia, D. A. U.S. Patent 4631337, 1986.

60. Newkome, G. R. U.S. Patent 5650101, 1998.

61. Bogart, G. R. U.S. Patent 5550063, 1996.

62. Peterson, B. "Hyperbranched Polyols - A Review of Development Work Performed at Perstorp Polyols." *Technical Data Brochure*, Perstorp, Sweden, January 1996.

63. DeSimone, J. M. "Branching Out Into New Markets." *Science*, vol. 269, 25 August 1995.

64. "Starburst Polymers." *Mechanical Engineering*, p. 60, August 1991.

65. O'Sullivan, D. A. "Dendrimers Nearing Availability for Commercial Evaluation." *C&EN*, 16 August 1993.

66. Salamone, J. C. "Encyclopedia of Polymeric Materials." CRC Press, vol. 3, 1996.

67. Frechet, J. M. "Dendrimers and Hyperbranched Polymers: Two Families of Three-Dimensional Macromolecules With Similar But Clearly Distinct Properties." *J. M. S. Pure Appl. Chem. A33*, vol. 10, pp. 1399–1425, 1996.

68. Khadir, A., and H. Gauthier. "Highly Branched Polymers as Melt Processing Additives." *ANTEC97 Proceedings*, p. 3732, 1997.

69. Uppuluri, S. "Rheology of Dendrimers. I. Newtonian Flow Behavior of Medium and Highly Concentrated Solutions of Polyamidoamine Dendrimers in Ethylenediamine Solvent." *Macromolecules*, vol. 31, p. 4498, 1998.

70. Massa, D., and K. A. Shriner. "Novel Blends of Hyperbranched Polyesters and Linear Polymers." *Macromolecules*, vol. 28, p. 3214, 1995.

71. Boogh, L., and B. Peterson. "Novel Tougheners for Epoxy-Based Composites." *SAMPE Journal*, vol. 33, January/February 1997.

72. Boogh, L., B. Petersson, and J. A. E. Månson. *Proceedings of the EPS Conf. Lausanne*, pp. 39–40, 1–6 June 1997, 1997.

73. *Perstorp Polyols Boltorn Material Data Brochure.* ????, ????, 1998.

74. ARCO Chemical Co. *Dylark Engineering Resins.* 1990.

75. Ashland Chemical Co. *General Polymers Materials Data Sheet.* 1997.

76. Beck Tan, N. C. "Morphology Control and Interfacial Reinforcement in Reactive Polystyrene/Amorphous Polyamide Blends." *Polymer*, vol. 37, no. 16, p. 3509, 1996.

77. Chang, F. "Styrene Maleic Anhydride and Styrene Glycidyl Methacrylate Copolymers as In-Situ Reactive Compatibilizers of Polystyrene/Nylon 6,6 Blends." *Polymer Engineering and Science*, vol. 31, no. 21, p. 1509, November 1991.

78. Dharmarajan, N. "Compatibilized Polymer Blends of Isotactic Polypropylene and Styrene Maleic Anhydride Copolymer." *Polymer*, vol. 36, no. 20, p. 3849, 1995.

79. Brannock, G. R. "Blends of Styrene Maleic Anhydride Copolymers With Polymethacrylates." *Journal of Polymer Science*, vol. 29, p. 413, 1991.

80. Simmons, A., and W. E. Baker. "Compatibility Enhancement in Polyethylene/Styrene Maleic Anhydride Blends Via Polar Interactions." *Polymer Communications*, vol. 31, p. 20, January 1990.

81. Brown, S. B. "Chemical Processes Applied to Reactive Extrusion of Polymers." *Annual Review of Material Science*, vol. 21, pp. 463–89, 1991.

82. Goodrich, J. E., and R. S. Porter. "A Rheological Interpretation of Torque Rheometer Data." *Polymer Engineering and Science*, January 1967.

83. White, J. L. *Principles of Polymer Engineering Rheology*, New York: Wiley and Sons, 1990.

84. Lin-Vien. *The Handbook of Infrared and Raman Characteristic Frequencies of Organic Molecules.* Academic Press Inc., 1991.

85. Majumdar, B., D. R. Paul, and A. J. Oshinski. "Evolution of Morphology in Compatibilized vs. Uncompatibilized Polyamide Blends." *Polymer*, vol. 38, issue 8, pp. 1787–1808, April 1997.

86. Fortelný, I., and A. Zivný. "Film Drainage Between Droplets During Their Coalescence in Quiescent Polymer Blends." *Polymer*, vol. 39, issue 12, pp. 2669–2675, June 1998.

87. Schoolenberg, G. E., and F. During. "Coalescence and Interfacial Tension Measurements for Polymer Melts: A Technique Using the Spinning Apparatus." *Polymer*, vol. 39, issue 4, pp. 757–763, February 1998.

88. Wu, S. *Polymer Engineering and Science*, vol. 30, no. 13, p. 753, 1990.

89. Bucknall, C. B. "Toughened Plastics." London: Applied Science Publishers, 1977.

90. Taylor, G. I. *Proc. Roy Soc. London*, vol. A146, p. 501, 1934.

91. Wu, S. "Formation of Dispersed Phase in Incompatible Polymer Blends: Interfacial and Rheological Effects." *Polymer Engineering and Science*, vol. 27, p. 335, 1987.

92. Ajji, A., and L. A. Utracki. "Interphase and Compatibilization of Polymer Blends." *Polymer Engineering and Science*, vol. 36, no. 12, June 1996.

93. Ward, I. M., and D. W. Hadley. "An Introduction to the Mechanical Properties of Solid Polymers." New York: Wiley and Sons, 1993.

94. Starke, J. U., and G. H. Michler. "Fracture Toughness of Polypropylene Copolymers: Influence of Interparticle Distance and Temperature." *Polymer*, vol. 39, issue 1, pp. 75–82, January 1998.

NO. OF COPIES	ORGANIZATION	NO. OF COPIES	ORGANIZATION
2	DEFENSE TECHNICAL INFORMATION CENTER DTIC DDA 8725 JOHN J KINGMAN RD STE 0944 FT BELVOIR VA 22060-6218	1	DIRECTOR US ARMY RESEARCH LAB AMSRL D R W WHALIN 2800 POWDER MILL RD ADELPHI MD 20783-1145
1	HQDA DAMO FDQ D SCHMIDT 400 ARMY PENTAGON WASHINGTON DC 20310-0460	1	DIRECTOR US ARMY RESEARCH LAB AMSRL DD J J ROCCHIO 2800 POWDER MILL RD ADELPHI MD 20783-1145
1	OSD OUSD(A&T)/ODDDR&E(R) R J TREW THE PENTAGON WASHINGTON DC 20301-7100	1	DIRECTOR US ARMY RESEARCH LAB AMSRL CS AS (RECORDS MGMT) 2800 POWDER MILL RD ADELPHI MD 20783-1145
1	DPTY CG FOR RDE HQ US ARMY MATERIEL CMD AMCRD MG CALDWELL 5001 EISENHOWER AVE ALEXANDRIA VA 22333-0001	3	DIRECTOR US ARMY RESEARCH LAB AMSRL CI LL 2800 POWDER MILL RD ADELPHI MD 20783-1145
1	INST FOR ADVNCD TCHNLGY THE UNIV OF TEXAS AT AUSTIN PO BOX 202797 AUSTIN TX 78720-2797		ABERDEEN PROVING GROUND
1	DARPA B KASPAR 3701 N FAIRFAX DR ARLINGTON VA 22203-1714	4	DIR USARL AMSRL CI LP (305)
1	NAVAL SURFACE WARFARE CTR CODE B07 J PENNELLA 17320 DAHLGREN RD BLDG 1470 RM 1101 DAHLGREN VA 22448-5100		
1	US MILITARY ACADEMY MATH SCI CTR OF EXCELLENCE DEPT OF MATHEMATICAL SCI MAJ M D PHILLIPS THAYER HALL WEST POINT NY 10996-1786		

NO. OF
COPIES ORGANIZATION

       ABERDEEN PROVING GROUND

20   DIR USARL
       AMSRL WM MA
         T J MULKERN (10 CPS)
         N C BECK TAN (10 CPS)

REPORT DOCUMENTATION PAGE

1. AGENCY USE ONLY (Leave blank)	2. REPORT DATE	3. REPORT TYPE AND DATES COVERED
	January 1999	Final, Jun 97 - Oct 98

4. TITLE AND SUBTITLE

Polystyrene/Hyperbranched Polyester Blends and Reactive
Polystyrene/Hyperbranched Polyester Blends

5. FUNDING NUMBERS

0601102A
AH42

6. AUTHOR(S)

Thomas J. Mulkern and Nora C. Beck Tan

7. PERFORMING ORGANIZATION NAME(S) AND ADDRESS(ES)

U.S. Army Research Laboratory
ATTN: AMSRL-WM-MA
Aberdeen Proving Ground, MD 21005-5069

8. PERFORMING ORGANIZATION REPORT NUMBER

ARL-TR-1876

9. SPONSORING/MONITORING AGENCY NAMES(S) AND ADDRESS(ES)

10. SPONSORING/MONITORING AGENCY REPORT NUMBER

11. SUPPLEMENTARY NOTES

12a. DISTRIBUTION/AVAILABILITY STATEMENT

Approved for public release; distribution is unlimited.

12b. DISTRIBUTION CODE

13. ABSTRACT (Maximum 200 words)

Newly developed hyperbranched polyols (HBP) possess a highly branched three-dimensional structure and a high density of functional end groups relative to conventional linear or branched polymer molecules. Due to their inherent low viscosity and versatile end group chemistry, these materials are attractive as polymer blend modifiers for improved processing as well as improved properties due to reactive compatibilization. In this work, the incorporation of HBPs in thermoplastic blends was investigated. Several volume fractions of hydroxyl functionalized hyperbranched polyesters were melt blended with nonreactive polystyrene (PS) and two types of reactive styrene maleic anhydride (SMA). Rheological data proved that HBPs are effective processing aids in both nonreactive and reactive blends. Studies including microscopy, thermal analysis, dynamic mechanical analysis, and Fourier transform infrared (FTIR) indicate that PS and HBP form an immiscible blend while SMA and HBP form compatibilized blends. The degree of compatibilization in the blends was found to increase with SMA reactivity.

14. SUBJECT TERMS

hyperbranched, dendrimer, reactive processing

15. NUMBER OF PAGES

61

16. PRICE CODE

17. SECURITY CLASSIFICATION OF REPORT	18. SECURITY CLASSIFICATION OF THIS PAGE	19. SECURITY CLASSIFICATION OF ABSTRACT	20. LIMITATION OF ABSTRACT
UNCLASSIFIED	UNCLASSIFIED	UNCLASSIFIED	UL

USER EVALUATION SHEET/CHANGE OF ADDRESS

This Laboratory undertakes a continuing effort to improve the quality of the reports it publishes. Your comments/answers to the items/questions below will aid us in our efforts.

1. ARL Report Number/Author_____ ARL-TR-1876 (Mulkern) _____ Date of Report __January 1999_____

2. Date Report Received _____

3. Does this report satisfy a need? (Comment on purpose, related project, or other area of interest for which the report will be used.) _____

_____

_____

4. Specifically, how is the report being used? (Information source, design data, procedure, source of ideas, etc.) _____

_____

_____

5. Has the information in this report led to any quantitative savings as far as man-hours or dollars saved, operating costs avoided, or efficiencies achieved, etc? If so, please elaborate. _____

_____

_____

6. General Comments. What do you think should be changed to improve future reports? (Indicate changes to organization, technical content, format, etc.) _____

_____

_____

_____

CURRENT
ADDRESS

Organization _____

Name _____ E-mail Name _____

Street or P.O. Box No. _____

City, State, Zip Code _____

7. If indicating a Change of Address or Address Correction, please provide the Current or Correct address above and the Old or Incorrect address below.

OLD
ADDRESS

Organization _____

Name _____

Street or P.O. Box No. _____

City, State, Zip Code _____

(Remove this sheet, fold as indicated, tape closed, and mail.)
(DO NOT STAPLE)